

Journal Pre-proof

1,2,3-Triazole-Chalcone hybrids: Synthesis, *in vitro* cytotoxic activity and mechanistic investigation of apoptosis induction in multiple myeloma RPMI-8226

Heba F. Ashour, Laila A. Abou-zeid, Magda A. -A. El-Sayed, Khalid B. Selim



PII: S0223-5234(20)30029-5

DOI: <https://doi.org/10.1016/j.ejmech.2020.112062>

Reference: EJMECH 112062

To appear in: *European Journal of Medicinal Chemistry*

Received Date: 12 November 2019

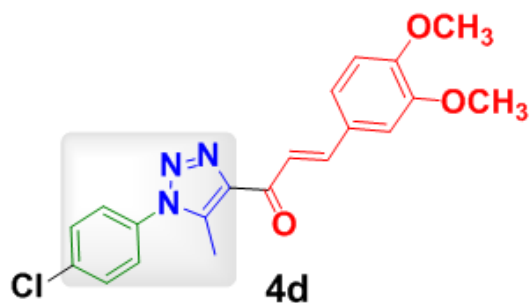
Revised Date: 8 January 2020

Accepted Date: 9 January 2020

Please cite this article as: H.F. Ashour, L.A. Abou-zeid, M.A.-A. El-Sayed, K.B. Selim, 1,2,3-Triazole-Chalcone hybrids: Synthesis, *in vitro* cytotoxic activity and mechanistic investigation of apoptosis induction in multiple myeloma RPMI-8226, *European Journal of Medicinal Chemistry* (2020), doi: <https://doi.org/10.1016/j.ejmech.2020.112062>.

This is a PDF file of an article that has undergone enhancements after acceptance, such as the addition of a cover page and metadata, and formatting for readability, but it is not yet the definitive version of record. This version will undergo additional copyediting, typesetting and review before it is published in its final form, but we are providing this version to give early visibility of the article. Please note that, during the production process, errors may be discovered which could affect the content, and all legal disclaimers that apply to the journal pertain.

© 2020 Published by Elsevier Masson SAS.



IC₅₀ values less than 1 μ M on 6 cancer cell lines

High Selectivity Index (SI)

Cell Cycle Arrest at G2/M phase

Trigger mitochondrial apoptotic pathway:

-Accumulation of ROS

-Up regulation of BAX

-Down regulation of Bcl-2

-Activation of caspases 3, 7, 9

Drug-likeness properties

Easy synthesis with good yield

1,2,3-Triazole-Chalcone hybrids: synthesis, *in vitro* cytotoxic activity and mechanistic investigation of apoptosis induction in multiple myeloma RPMI-8226

Heba F. Ashour^{1,2}, Laila A. Abou-zeid^{1,3}, Magda A. -A. El-Sayed^{*,1,2}, Khalid B. Selim^{*,1}

¹Department of Pharmaceutical Organic Chemistry, Faculty of Pharmacy, Mansoura University, Mansoura 35516, Egypt.

²Department of Pharmaceutical Chemistry, Faculty of Pharmacy, Horus University, New Dammeitta, Egypt.

³Department of Pharmaceutical Chemistry, Faculty of Pharmacy, Delta University, Gamsaa, Egypt.

*Corresponding author: M. A. -A. El-Sayed (e-mail: magdaaziz1@yahoo.com) and K. B. Selim (e-mail: khbselim@mans.edu.eg)

tel: +2050-2247496 fax: +2050-2247496

Abstract

A new series of 1,2,3-triazole-chalcone hybrids has been synthesized and screened *in vitro* against a panel of 60 human cancer cell lines according to NCI (USA) protocol. Compound **4d** having 3, 4-dimethoxyphenyl chalcone moiety, the most potent derivative, inhibited the growth of RPMI-8226 and SR leukemia cell lines by 99.73% and 94.95% at 10 μ M, respectively. Also, it inhibited the growth of M14 melanoma, K-562 leukemia, and MCF7 breast cancer cell lines by more than 80% at the same test concentration. **4d** showed IC₅₀ values less than 1 μ M on six types of tumor cells and high selectivity index reached to 104 fold on MCF7. Compound **4d** showed superior activity than methotrexate and gefitinib against the most sensitive leukemia cell lines in addition to higher or comparable activity against the rest sensitive cell lines. Flow cytometry analysis in RPMI-8226 cells revealed that compound **4d** caused cell cycle arrest at G2/M phase and induced apoptosis in a dose dependant manner. Mechanistic evaluation referred this apoptosis induction to triggering mitochondrial apoptotic pathway through inducing ROS accumulation, increasing Bax/Bcl-2 ratio and activation of caspases 3, 7 and 9.

Keywords Antiproliferative activity, 1,2,3-triazole, chalcone, cell cycle analysis, apoptosis, ROS, NCI-60

1. Introduction

Cancer is a life threatening disease and is the major cause of death throughout the world [1]. Development of effective cancer therapies, based on preventing cell proliferation and/or inducing apoptosis, is a great challenge to the researchers. Despite major advances, multiple myeloma (MM) remains an incurable malignancy. MM is a hematologic malignancy characterized by a clonal expansion of plasma cells in bone marrow, accounting for 1% of all malignancies and 10% of hematologic malignancies [2]. Combination therapy has been used as an initial treatment for MM patients and involves normally two or three anti-myeloma drugs which have different mechanisms of action and work synergistically including alkylating agents such as melphalan or cyclophosphamide, corticosteroids such as prednisolone or dexamethasone, proteasome inhibitors such as bortezomib, carfilzomib or ixazomib and recent approved drugs (Figure 1) such as venetoclax as Bcl-2 inhibitor, panobinostat as histone deacetylase (HDAC) inhibitor or selinexor as nuclear export inhibitor [3]. Even though those treatments improved the outcome of MM patients, MM often remains incurable due to the

development of drug resistance governed by the bone marrow microenvironment [4]. Therefore, targeting new pathways, *via* synthesis of chemotherapeutics as small molecules, is needed to overcome this resistance and to increase their potency.

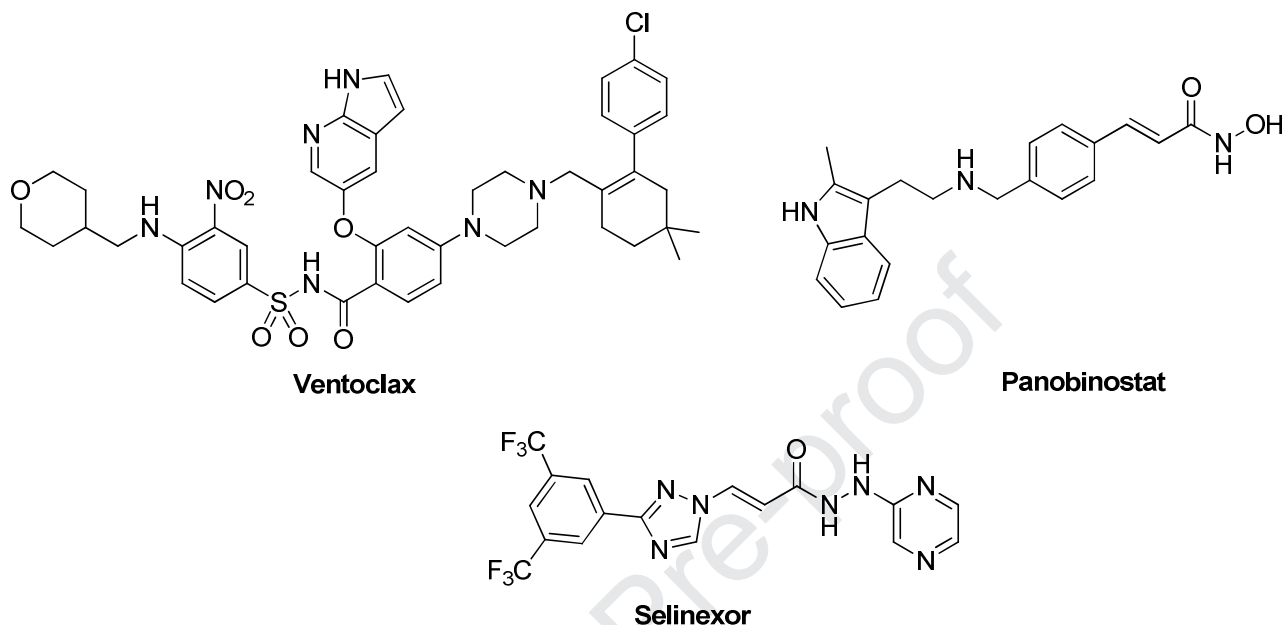


Figure 1. Drugs approved in the treatment of multiple myeloma

Several studies have introduced many mechanisms, in treatment of leukemia, triggered to induce anti-proliferative effect against MM RPMI-8226 cells, including: i) down regulation of the expression of HDACs such as HDAC1, HDAC2, HDAC3 and HDAC6 [5, 6, 7]; ii) inhibition of nuclear factor-kappa B (NF- κ B) [8, 9]; iii) inhibition of epidermal growth factor receptors (EGFRs) family [10]; iv) regulation of Bcl-2 and Bax as well as suppression of vascular endothelial growth factors (VEGFs) [11]; v) direct binding to microtubules in endothelial cells [12]; vi) disturbing the mitochondrial pathway [13] and *via* accumulation of reactive oxygen species (ROS) [14].

Chalcone is an α,β -unsaturated ketone that represented a central core for a variety of important bioactive molecules which possess versatile biological activities including anticancer [15], antimicrobial [16], antituberculosis [17], antiinflammatory [18], antioxidant [19], antimalarial [20], antidiabetic [21] and antihypertensive [22]. Structural modification of chalcones was proved to be successful strategy in developing new anticancer agents differ in their potency and mechanism of action as a result of various interactions with various target proteins related to cytotoxic activity such as HDACs, EGFRs, VEGFRs, microtubules, topoisomerases, NF- κ B. [23]. Furthermore, it was well-explored that compounds containing chalcone moiety induce apoptosis and cell cycle arrest at G2/M phase by triggering mitochondrial apoptotic pathway through activation of caspases and elevation of Bax/Bcl-2 ratio [24]. For example, as shown in Figure 2, Flavokawain B [25] was reported to induce G2/M cell-cycle arrest and apoptosis in human oral and gastric carcinoma through generation of intracellular ROS. Isobavachalcone [26] and JAI-51 [27] were reported to induce apoptotic cell death through increasing Bax/Bcl-2 ratio and activation of caspases 3 and 9 in the mitochondrial pathway. MBL-II-58 [27] was

reported to induce ROS production and autophagic cell death. Moreover, triazolyl [28] and quinolyl-thienyl chalcones [29] were reported as antitubulin and antiangiogenic agents, respectively.

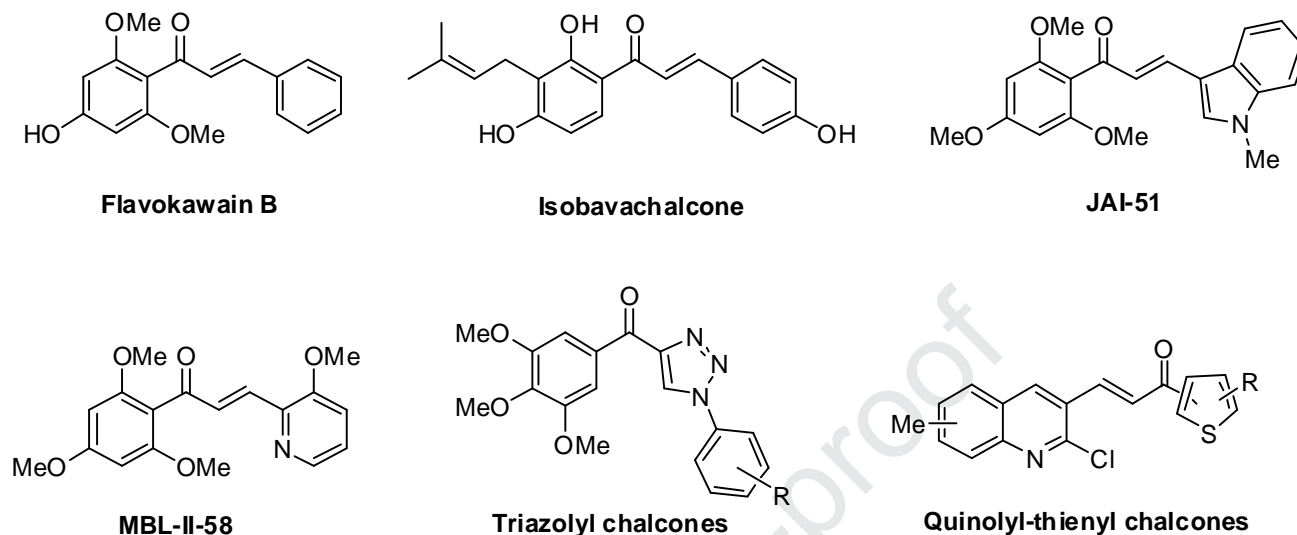


Figure 2. Chalcone derivatives with anticancer activity.

Furthermore, 1,2,3-triazoles have attained considerable attention owing to their diverse biological activities, attractive physicochemical properties and ease of synthesis [30]. 1,2,3-Triazole is one of the key structural units found in a large variety of bioactive molecules including anticancer, antimicrobial, antifungal, antiviral, antiparasitic, antitubercular, antidiabetic, antiinflammatory, analgesic, anticonvulsant, antidepressant [31]. These azoles have the ability to bind to different biological targets (e.g. receptors and enzymes) by diverse non-covalent interactions [31]. In addition, 1,2,3-triazole ring is highly stable to metabolic degradation and can be used as a bioisostere for amide bond, disulphide bond, ester bond, carboxylic acid, aromatic rings and olefins rigid analogs [32].

Based on the earlier findings, molecular hybridization between chalcones and different bioactive heterocyclic moieties was carried out in an attempt to get new effective anticancer molecules with increased selectivity, lower drug resistance and/or less side effects. Thus, in the current work, hybridization between the chalcone moiety of Flavokawain B and the bioactive 1,2,3-triazole core was performed to give novel bioactive hybrids (Figure 3). All the synthesized compounds were evaluated for their *in vitro* antiproliferative activities against a panel of NCI-60 cancer cell lines. The most potent compound was further investigated to measure its apoptotic effect and to discover its mechanistic pathway through measuring its effect on HDACs, NF- κ B, EGFR, VEGFR, topoisomerase 2, tubulin, Bax, Bcl-2, PARP-1, caspases 3, 7, 9 and ROS in leukemia RPMI-8226 cells.

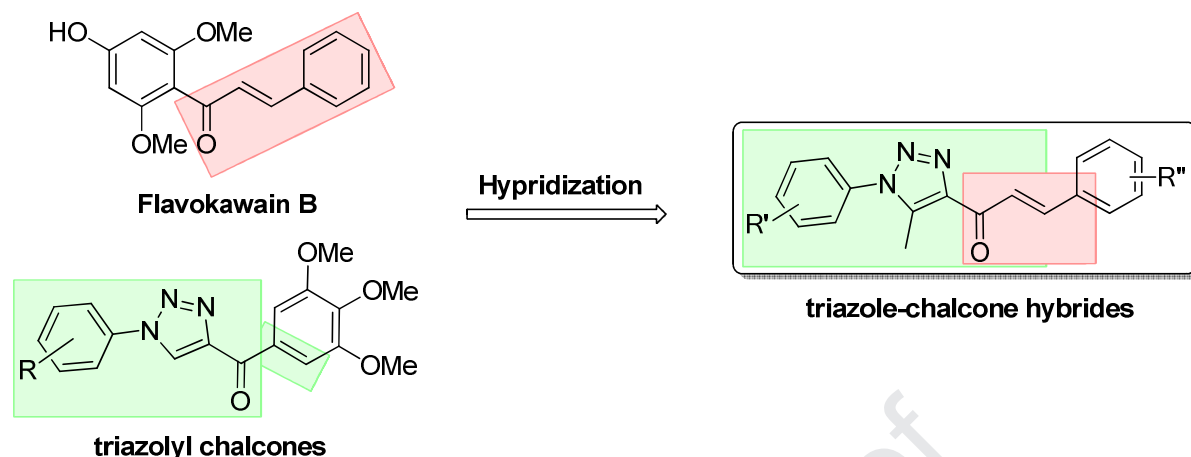
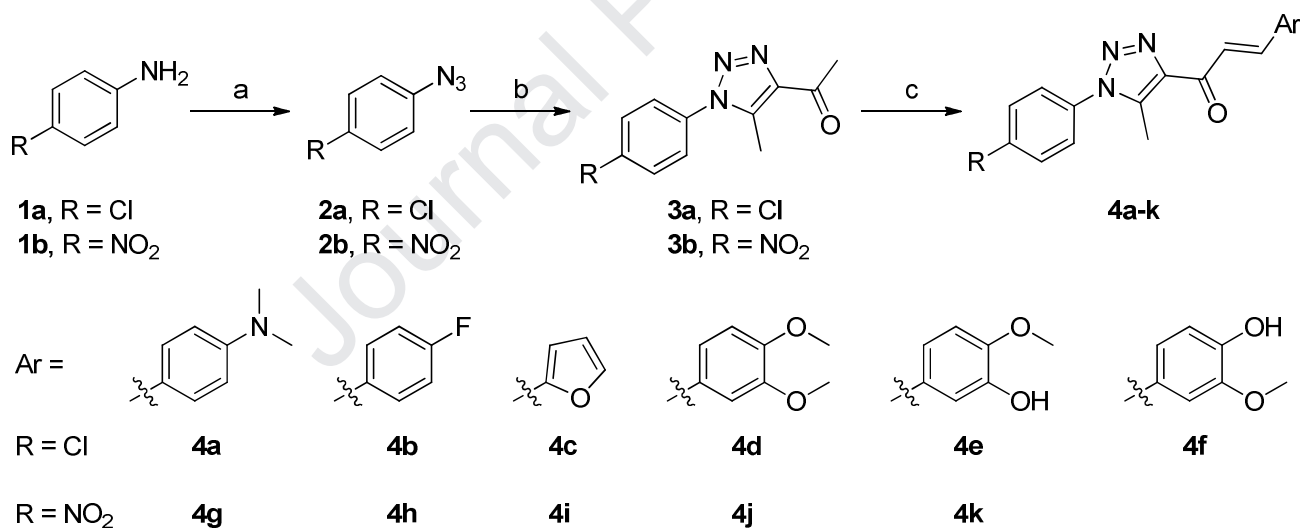


Figure 3. Molecular hybridization of chalcone scaffold with 1,2,3-triazole.

2. Results and discussion

2.1. Chemistry



Scheme 1. Synthesis of hybrids **4a–k**. Reagents and conditions: (a) HCl/NaNO₂, 0 °C; NaN₃; (b) acetylacetone, Na, MeOH, rt, 24 h; (c) Ar-CHO, NaOH, EtOH, rt, 24-72 h.

As depicted in Scheme 1, the starting aryl azides **2a, b** were prepared according to the reported methods [33] *via* the reaction of the corresponding aryl amine **1a, b** with sodium nitrite under acidic condition at 0 °C followed by treating with sodium azide. The chloroazide **2a** was extracted by ethyl acetate after 24 h of stirring, while the nitroazide **2b** precipitated from the reaction mixture. The key intermediates, acetyl 1,2,3-triazoles **3a, b** were prepared by treating the azides **2a, b** with acetylacetone in presence of sodium methoxide [34]. The target triazole-chalcone hybrids **4a–k** were synthesized by conventional aldol condensation between aromatic aldehydes (e.g. 4-dimethylaminobenzaldehyde, 4-

flourobzaldehyde, furfural, 3,4-dimethoxybenzaldehyde, isovanillin or vanillin) and acetyl triazole derivatives **3a, b** in presence of ethanolic solution of sodium hydroxide. New hybrids were produced in 46–92% yield as pure compounds and their structures were characterized by spectroscopic analysis (^1H and ^{13}C -NMR) as described in the experimental section.

2.2. Biological evaluation

2.2.1. *In vitro* one-dose antiproliferative screening

The newly synthesized hybrids **4a–k** were screened against a panel of 60 cell lines of different cancer types (leukemia, non small cell lung cancer, colon cancer, CNS cancer, melanoma, ovarian cancer, renal cancer, prostate cancer and breast cancer) at the National Cancer Institute (NCI), USA [35] in order to detect their growth inhibition percentages (GI%) at a single dose concentration (10 μM) on cancer cell lines. Additionally, the selectivity ratio on a particular cell line with regard to all NCI-60 cell line (Table 1) was recorded.

Data analysis of growth inhibition assay showed that the majority of the compounds exhibited potent anticancer activity against leukemia cell lines rather than other cell lines. Compounds **4d** and **4f** have broad spectrum cytotoxic activity against the tested cell lines, particularly against leukemia cell lines. Compounds **4b** and **4h** showed potent activity against leukemia cell line RPMI-8226 with GI% of 88 and 86, respectively. Compound **4i** showed high activity against leukemia CCRF-CEM with GI% value of 81. The rest of the tested compounds **4c, 4e, 4g, 4j** and **4k** showed low to moderate growth inhibitory activities. Compound **4d** has excellent activity against leukemia cell lines (K-562, RPMI-8226, SR), melanoma M14 and breast MCF7 cell lines with GI% range of 82–100; colon cancer HCT-116 and prostate cancer PC-3 with GI% values of 68 and 60, respectively. Moreover, compound **4f** showed moderate to high activity against leukemia cell lines with GI% range of 47–92; however, inhibitory activity for colon cancer HCT-116 and breast cancer MCF7 are 74 and 73, respectively.

Many tested hybrids showed high potency with great selectivity on specific cell lines. For example, compounds **4b** and **4h** having *para* fluoro phenyl-chalcone moiety showed strong GI% against leukemia RPMI-8226 cell line of 88% and 86%, respectively, with high selectivity ratio equal to 11.95 fold and 7.51 fold, respectively. While, compound **4i** with furfuryl-chalcone moiety showed strong GI% against leukemia CCRF-CEM cell line equal to 81.25% with remarkable selectivity ratio of 12.48 fold. Compound **4f** having *para* hydroxy and *meta* methoxy groups on the phenyl-chalcone moiety showed strong GI% over 4 cell lines (leukemia HL-60 (TB), leukemia CCRF-CEM, colon HCT-116 and breast cancer MCF7) equal to 92.41%, 76.46%, 73.77% and 73.16%, respectively, with selectivity ratio around 3 fold with regard to all NCI-60 cell lines. It also exerted good activity over K-562, RPMI-8226 and SR leukemia cell lines with GI% values of 65.06%, 57.21% and 56.22%, respectively. Compound **4d** possessing 3, 4-dimethoxyphenyl chalcone moiety was the most active in our series. It showed strong GI% over 5 cell lines, RPMI-8226 leukemia, SR leukemia, K-562 leukemia, M14 melanoma and MCF7 breast cancer cell lines reached to 99.73%, 94.95% , 83.17%, 87.26% and 81.97%, respectively, with selectivity ratio of around 3 fold with regard to all NCI-60 cell lines. It also exerted good activity against HCT-116 colon and PC-3 prostate cancer cell lines with GI% values of 68.01% and 59.88%, respectively.

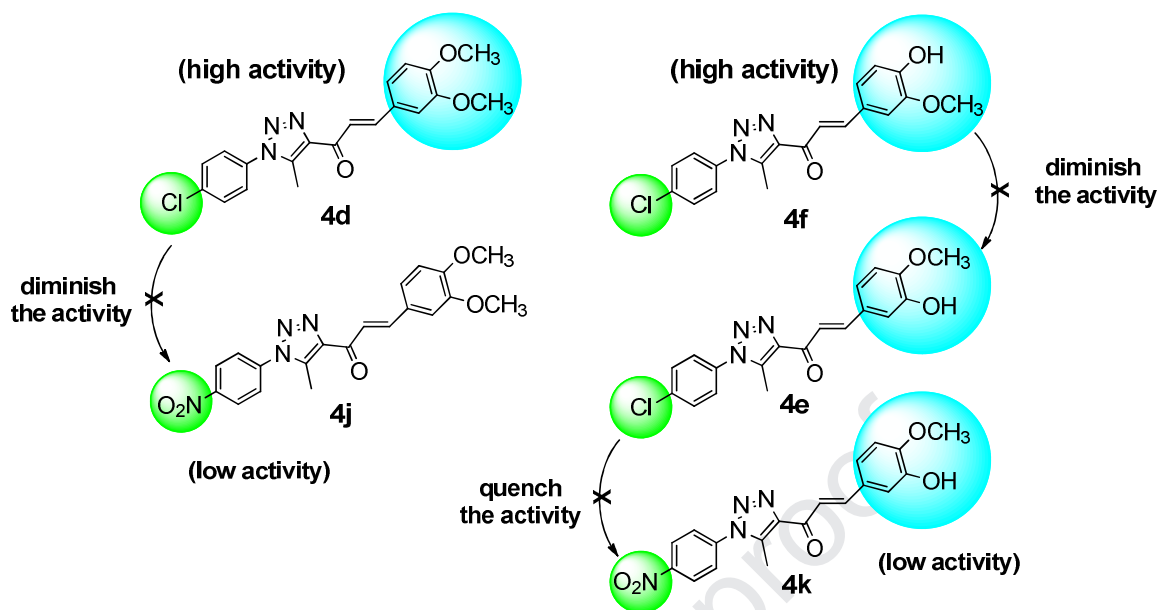


Figure 4. SAR study of triazole-chalcone hybrids.

As illustrated in Figure 4, the results showed that the derivatives substituted with the weak electron withdrawing chloro atom were more potent cytotoxic agents than the derivatives substituted with the strong electron withdrawing nitro group, particularly the *para* chloro compound **4d** exhibited the highest % mean of inhibition value over the 60 cell line panel equal to 27.19% in comparison to the *para* nitro compound **4j** which exhibited 3.15%. Moreover, switching the positions of the high polar OH and the less polar OCH₃ groups (from *para* to *meta* position and *vice versa*) on the phenyl ring of **4f** and **4e** led to diminish the % mean of inhibition from 25% (for **4f**) to 4.9% (for **4e**), indicating the important cytotoxic effect of the *meta* position of OCH₃ group in **4f**. Confirming the importance of the *para* chloro substituent, replacing Cl atom in **4e** with NO₂ group in the corresponding **4k** quenched the activity to give the weakest active compound among the series with 0.23% mean of inhibition. Such results suggest that the electronic and steric properties of the substituents play an important role in the binding affinity of chalcones to their cellular target(s). As a general statement, the presence of *meta* OCH₃ group on the right side and *para* Cl atom on the left side of the hybrid was proved to be essential for general anticancer activity of the tested series.

Table 1. Percentages of growth inhibition (GI%) induced by the synthesized compounds at 10 μM concentration on NCI-60 cell line panel and the selectivity ratio on the most sensitive cell lines.

Subpanel cancer cell Lines	%Growth Inhibition (GI%)										
	4a	4b	4c	4d	4e	4f	4g	4h	4i	4j	4k
Leukemia											
CCRF-CEM	33.21	36.91	24.22	49.25	9.43	76.46	8	14.54	81.25	6.93	2.79
HL-60(TB)	28.32	16.87	24.76	54.02	11.46	92.41	11.73	17.1	4.69	9.18	2.33
K-562	26.26	15.71	21.83	83.17	13.62	65.06	14.49	27.56	NI	14.44	2.1
MOLT-4	14.29	20.52	17.03	38.68	9.29	47.54	18.76	13.33	1.37	14.3	2.76

RPMI-8226	37.68	87.98	28.66	99.73	5.17	57.21	4.01	86.33	1.48	16.28	2.91
SR	20.18	32.7	47.33	94.95	6.88	56.22	20.08	45.42	6.38	26.25	NI
Non-Small Cell Lung Cancer											
NCI-H226	0.33	10	4.87	30.04	0.65	8.63	11.14	8.05	7.01	5.6	1.01
Colon Cancer											
HCT-116	1.84	7.49	10.33	68.01	13.03	73.77	11.4	17.07	46.87	0.38	1.94
HCT-15	3.93	10.91	18.86	41.06	NI	46.43	6.51	22.04	4.18	4.22	4.58
HT29	11.26	10.15	11.67	34.27	NI	41.02	5.08	16.28	NI	0.02	NI
KM12	6.53	15.9	8.74	45.77	4.95	41.55	5.65	2.25	3.34	11.1	NI
SW-620	NI	NI	NI	33.06	1.27	30.27	NI	3.65	NI	0.25	2.31
Melanoma											
LOX IMVI	NI	NI	NI	29.66	7.01	44.44	3.18	9.16	NI	NI	2.26
M14	18.22	17.59	13.88	87.26	9.47	27.64	9.34	26.01	35.83	14.86	0.76
MDA-MB-435	NI	NI	NI	32.02	7.48	50.78	NI	1.35	NI	NI	3.68
SK-MEL-5	NI	NI	NI	31.88	2.34	4.89	NI	1.21	NI	NI	1
UACC-62	11.05	26.54	25.37	41.17	12.88	30.69	12.06	40.12	15.31	16.48	8.53
Ovarian Cancer											
IGROV1	NI	NI	2.31	30.18	5.46	20.34	NI	2.58	NI	NI	0.39
OVCAR-3	NI	NI	NI	15.51	NI	37.43	NI	NI	NI	NI	NI
Renal Cancer											
786-0	NI	7.6	14.4	12.84	6.45	9.61	9.25	11.89	34.18	NI	3.95
CAKI-1	6.13	3.19	NI	12.45	15.48	42.24	3.23	8.5	4.27	8.22	10.47
SN12C	7.26	5.68	10.37	23.47	9.17	31.46	9.61	6.13	10.97	4.45	9.41
UO-31	27.77	14.85	19.79	34.16	24	46.69	25.34	40.87	22.04	18.72	20.15
Prostate Cancer											
PC-3	24.15	23.53	9.34	59.88	10.42	36.7	13.59	15.68	4.68	11.94	6.01
Breast Cancer											
MCF7	27.28	33.47	28.59	81.97	7.2	73.16	3.84	54.72	13.08	13.32	5.23
BT-549	7.35	5.6	9.01	43.99	6.1	29.45	18.02	15.07	35.18	10.32	NI
T-47D	16.45	17.78	15.52	32.11	15.43	27.51	10.32	17.19	12.33	9.88	2.17
MDA-MB-468	NI	NI	8.02	33.89	1.68	27.03	NI	5.39	1.12	NI	0.41
Mean Inhibition											
	4.78	7.36	7.9	27.19	4.9	25	6.28	11.5	6.51	3.15	0.23
Selectivity Ratio on the Most sensitive Cell Line (GI% on the sensitive cell line/Mean Inhibition)											
CCRF-CEM	-----	-----	-----	-----	-----	3.06	-----	-----	12.48	-----	-----
HL-60(TB)	-----	-----	-----	-----	-----	3.70	-----	-----	-----	-----	-----
K-562	-----	-----	-----	3.06	-----	-----	-----	-----	-----	-----	-----
MOLT-4	-----	-----	-----	-----	-----	-----	-----	-----	-----	-----	-----
RPMI-8226	-----	11.95	-----	3.67	-----	-----	-----	7.51	-----	-----	-----
SR	-----	-----	-----	3.49	-----	-----	-----	-----	-----	-----	-----
HCT-116	-----	-----	-----	-----	-----	2.95	-----	-----	-----	-----	-----
M14	-----	-----	-----	3.21	-----	-----	-----	-----	-----	-----	-----
MCF7	-----	-----	-----	3.01	-----	2.93	-----	-----	-----	-----	-----

*The bold red and blue figures indicate strong (GI% > 70%) and moderate (GI% 30-70%) anticancer activity, respectively; NI, no inhibition.

*Non sensitive cell lines which show GI% < 30% for all synthesized compounds were not mentioned.

*Mean inhibition and selectivity ratio were calculated with regard to GI% values over all NCI-60 cell lines.

Figure 5 shows the cytotoxic effect of *para* chloro substituent *versus para* nitro substituent for compounds **4d** and **4j** towards the most sensitive cell lines in comparison to methotrexate and gefitinib as reference drugs. The cytotoxic activity of the reference drugs was obtained from NCI data ware house index [36]. Compound **4d** showed higher activity than methotrexate and gefitinib against the leukemia cell lines RPMI-8226, SR and K-562. Moreover, it showed higher or comparable activity against breast MCF7, colon HCT-116, prostate PC-3 and melanoma M14 cancer cell lines. These results indicate that compound **4d** can be considered as a potential lead compound for future development of broad spectrum anticancer agents.

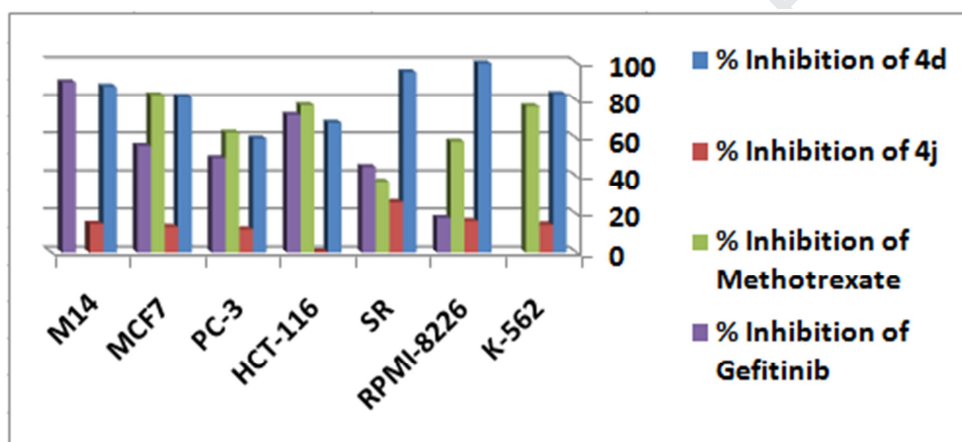


Figure 5. A comparison between **4d** (with chloro atom) and **4j** (with nitro group). GI % of *in vitro* subpanel tumor cell lines, **Leukemia:** K-562, RPMI-8226, SR, **Colon Cancer:** HCT-116, **Prostate Cancer:** PC-3, **Breast Cancer:** MCF7 and **Melanoma:** M14 in comparison to methotrexate and gefitinib.

2.2.2. *In vitro* cytotoxicity screening (IC_{50}) against cancer and human normal cell lines and selectivity index (SI)

As shown in Table 2, the IC_{50} of compounds **4b**, **4d**, **4f**, **4h** and **4i** were determined to assess their cytotoxic activity against several cancer cells *versus* corresponding human normal cells in order to evaluate their selectivity index (SI). It is accepted that the tested compound which has SI value more than three exhibits selective cytotoxicity towards the cancer cells rather than the normal cells, while the compound which has SI value less than three exhibits general toxicity for cancer and normal cells [37, 38]. The results showed that: i) compounds **4b** and **4h** exhibited IC_{50} values in nanomolar range against leukemia RPMI-8226 cell line as well as high SI values on cancer cells rather than normal cells equal to 114.43 folds and 45.19 folds, respectively; ii) compound **4i** also showed IC_{50} values in nanomolar range against leukemia CCRF-CEM cell line as well as high SI value of 103.6 folds; iii) compound **4f** showed IC_{50} values in nanomolar range over two cancer cell lines, HL(60)-TB leukemia and CCRF-CEM leukemia cell lines with high SI values of 27.1 folds and 14.26 folds, respectively. It also showed IC_{50} values in submicromolar range over two cancer cell lines, MCF7 breast and HCT-116 colon cancer cell lines with high SI values of 22.08 folds and 13.38 folds, respectively; iv) compound **4d**, the most potent

derivative, showed IC_{50} values in nanomolar range over six cancer cell lines, RPMI-8226 leukemia, SR leukemia, K-562 leukemia, M14 melanoma, MCF7 breast and HCT-116 colon cancer cell lines, and showed IC_{50} value in submicromolar range over PC-3 prostate cancer cell line, however, it showed much higher IC_{50} values (12.88 μ M to 30.09 μ M) on the corresponding normal cell lines indicating the high selectivity of compound **4d** towards cancer cells rather than normal cells reached to 45.53 folds in RPMI-8226 leukemia, 30.35 folds in SR leukemia, 34.69 folds in K-562 leukemia, 43.61 folds in M14 melanoma, 104.17 folds in MCF7 breast cancer, 65.96 folds in HCT-116 colon cancer and 4.37 folds in PC-3 prostate cancer. In summary, the results of cytotoxicity point to the potent broad spectrum anticancer activity with the high safety of compound **4d**.

Table 2. Cytotoxic activity (IC_{50} , μ M) and Selectivity Index (SI) of compounds **4b**, **4d**, **4f**, **4h** and **4i**.

Cytotoxicity of compound 4b				SI ^b
Cancer cells (IC_{50} , μ M) ^a		Normal cells (IC_{50} , μ M) ^a		
Leukemia RPMI-8226	0.49 \pm 0.02	Blood PCS-800-011	56.07 \pm 1.07	114.43
Cytotoxicity of compound 4d				SI ^b
Cancer cells (IC_{50} , μ M) ^a		Normal cells (IC_{50} , μ M) ^a		
Leukemia RPMI-8226	0.64 \pm 0.02	Blood PCS-800-011	29.14 \pm 1.4	45.53
Leukemia SR	0.96 \pm 0.04			30.35
Leukemia K-562	0.84 \pm 0.07			34.69
Melanoma M14	0.69 \pm 0.01	Skin WS1	30.09 \pm 1.7	43.61
Breast MCF7	0.24 \pm 0.01	Breast MCF 10A	25.00 \pm 1.1	104.17
Colon HCT116	0.26 \pm 0.01	Colon CCD-18	17.15 \pm 1.5	65.96
Prostate PC3	2.95 \pm 0.14	Prostate HPrEC	12.88 \pm 0.9	4.37
Cytotoxicity of compound 4f				SI ^b
Cancer cells (IC_{50} , μ M) ^a		Normal cells (IC_{50} , μ M) ^a		
Leukemia CCRF-CEM	0.76 \pm 0.01	Blood PCS-800-011	10.84 \pm 0.66	14.26
Leukemia HI-60 (TB)	0.40 \pm 0.005			27.1
Leukemia K-562	10.84 \pm 0.4			1
Breast MCF7	1.76 \pm 0.04	Breast MCF 10A	38.86 \pm 1.14	22.08
Colon HCT116	2.87 \pm 0.06	Colon CCD-18	38.39 \pm 0.95	13.38
Cytotoxicity of compound 4h (IC_{50} , μ M) ^a				SI ^b
Cancer cells (IC_{50} , μ M) ^a		Normal cells (IC_{50} , μ M) ^a		
Leukemia RPMI-8226	0.78 \pm 0.04	Blood PCS-800-011	35.25 \pm 0.81	45.19
Cytotoxicity of compound 4i				SI ^b
Cancer cells (IC_{50} , μ M) ^a		Normal cells (IC_{50} , μ M) ^a		
Leukemia CCRF-	0.45 \pm 0.008	Blood PCS-800-	46.62 \pm 1.23	103.6

CEM		011		
-----	--	-----	--	--

^aCytotoxicity (IC₅₀, μM): The concentration of compound that inhibit 50% of the cell growth after 48 h of drug exposure measured by MTT assay. Each value was shown as mean ± SD of three experiments; ^bSelectivity Index (SI) = IC₅₀ for normal cells/IC₅₀ for cancer cells.

2.2.3. Physicochemical properties and Lipinski's rule of five

The bioavailability of the compound determines its ability to cross the biological barriers in order to reach its target sites. It is influenced by many parameters such as solubility, membrane permeability, as well as active uptake and transport within the organism [39]. The “rule-of-five” introduced by Lipinski [40] summarized the molecular features and properties that are associated with orally active drugs in humans, and additional related criteria were added later on by Veber [41]. These parameters have been widely used as a filter for new potential drugs and the violation of more than one of these rules may indicate problems in the drug bioavailability. Therefore, the physicochemical parameters of compound **4d**, the most compound as anticancer, were predicted (Table 3) using Molinspiration software [42]. The calculation showed that compound **4d** complies with these rules which indicated the drug-likeness properties of this compound.

Table 3. Reference values of Lipinski's and Veber's rules as well as predicted physicochemical properties of compound **4d**, **4f** and Gefitinib.

	cLogP	MW	PSA	HBD	HBA	nRotB
Lipinski ^a	≤ 5	≤ 500	-	≤ 5	≤ 10	-
Veber ^b	-	-	≤ 140	-	-	≤ 10
Compound 4d ^c	3.79	383.83	66.26	0	6	6
Compound 4f ^c	3.48	369.81	77.25	1	6	5
Gefitinib	4.19	446.91	68.75	1	7	8

^aLipinski's rule of five for pharmaceuticals; ^bVeber added more criteria to Lipinski's rule of five; ^cPredicted physicochemical properties; cLogP: calculated lipophilicity; MW: molecular weight; PSA: polar surface area; HBD: number of hydrogen bond donor; HBA: number of hydrogen bond acceptor; nRotB: number of rotatable bounds.

2.2.4. Mechanistic investigation of inducing cytotoxicity in multiple myeloma RPMI-8226

Since compound **4d** showed high potency against leukemia cells, good safety profile and drug-likeness properties along with easy synthetic pathway (in only 3 steps), it is indicated that compound **4d** could be a promising lead for future development of active antileukemic agents. So, in this study, we focused our efforts to find out the biological target for compound **4d** inside RPMI-8226 cells and its mechanism of inducing cytotoxicity in order to offer new insights in treating MM. Therefore, we investigated the activity of compound **4d** on a variety of proteins and enzymes targets which previously reported to induce cytotoxicity in RPMI-8226 cell line as well as its effect on some proteins which regulate the cell cycle progression.

2.2.4.1. *In vitro* enzyme inhibition assays

As illustrated in Figure 6, we measured the activity of compound **4d** on class I HDACs (1, 2, 3 and 8) and class IIb (HDAC6) using velcade as a reference drug. The results showed that the effect of **4d** on several types of HDAC is weak except on HDAC8 as it shows high activity ($IC_{50} = 0.047 \mu M$) in comparison to velcade ($IC_{50} = 0.072 \mu M$). Moreover, the effect of compound **4d** against several molecular targets including NF- κ B, EGFR, VEGFR2, topoisomerase 2 and tubulin were screened where compound **4d** showed lower inhibitory activities in comparison to the reference drugs as shown in Figure 6. These results indicate that the previous enzymes and proteins might be not the molecular targets for 1,2,3-triazole-chalcone hybrid **4d** to induce cytotoxicity inside MM RPMI-8226 cells.

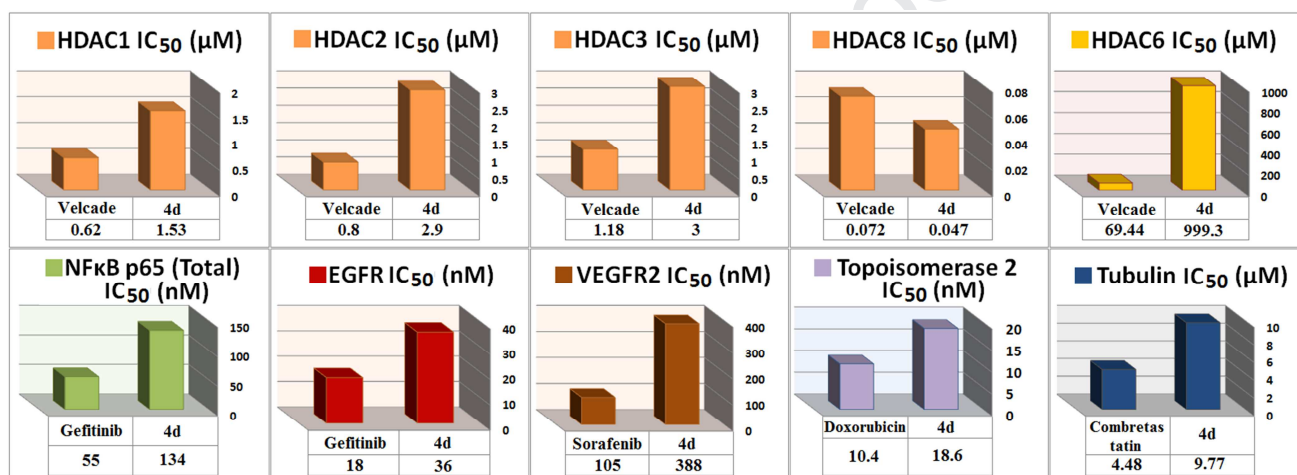


Figure 6. Assessment of activity of compound **4d** against HDACs, NF- κ B, EGFR, VEGFR2, topoisomerase 2 and tubulin in RPMI-8226 cells. HDAC, histone deacetylase; NF- κ B, nuclear factor kappa B; EGFR, epidermal growth factor receptor; VEGFR, vascular endothelial growth factor receptor.

2.2.4.2. *Measuring the expression of apoptotic and anti-apoptotic markers*

Permeabilization of mitochondrial outer membrane is controlled by a balance between the proteins of the Bcl-2 family [43], which composed of pro-apoptotic proteins such as Bax, Bim, Bad, Bid and Puma and anti-apoptotic proteins such as Bcl-2, Mcl-1 and Bcl-XL [44, 45]. In human MM, the chemoresistance correlates with elevated levels of Bcl-2 which is commonly observed in this disease [46, 47]. Also, Apoptosis is known to be inhibited when Bcl-2 increases and forms a Bcl-2–Bax heterodimer, and induced when Bax increases and forms a homodimer [48]. Bax homodimers can increase mitochondrial membrane permeability and leakage of cytochrome C into the cytoplasm, resulting in a caspase dependent apoptosis [49] in which caspase-9 is activated and leads naturally to caspase-3 activation in the latter [50] which in turn induces apoptosis that can be identified by the proteolytical cleaved caspase-3 and caspase-7 [51]. Based on that, as shown in, Figure 7, the study was further extended to investigate the effect of compound **4d** to provoke apoptosis by affecting the expression of apoptotic and anti-apoptotic markers in RPMI-8226 cells. Compound **4d** significantly increased the expression levels of

the active apoptotic markers including caspase-3, caspase-7, caspase-9 and Bax by about 100, 4.5, 8.5, 5.3 folds, respectively, in comparison to the control. Moreover, **4d** strongly decreased the level of the anti-apoptotic marker Bcl-2. These results showed the activation of caspase-9 which is the upstream of caspases-3 and 7, besides the down regulation of Bcl-2 and upregulation of Bax leading to elevated Bax/Bcl-2 ratio suggests that compound **4d** induces apoptosis in human MM RPMI-8226 cells through mitochondrial-mediated pathway (Figure 8).

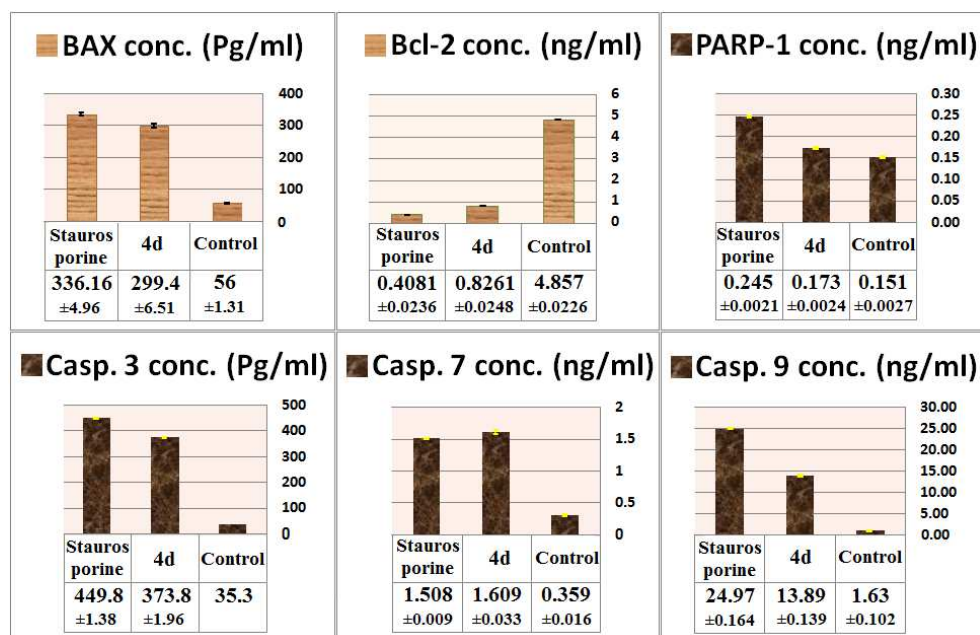


Figure 7. Assessment of activity of compound **4d** against Bax, Bcl-2, PARP-1 and Casp. 3, 7, 9 in RPMI-8226 cells. Casp., Caspase; PARP-1, poly (ADP-ribose) polymerase.

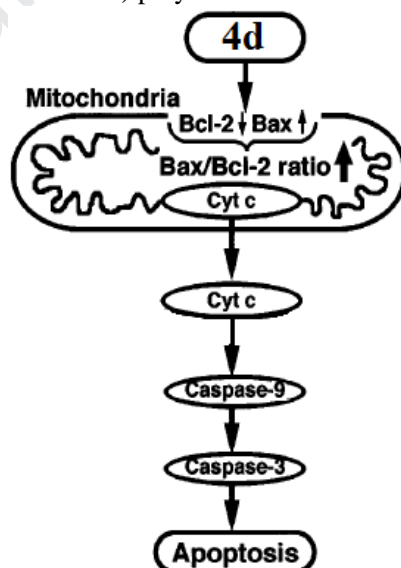


Figure 8. Effect of compound **4d** on apoptosis *via* mitochondrial-mediated pathway in RPMI-8226 cells.

2.2.4.3. Intracellular ROS accumulation assay

Reactive oxygen species (ROS) such as H_2O_2 and superoxide can cause cytochrome c (Cyt c) release from mitochondria and induce apoptosis through the mitochondrial pathway [52]. As illustrated in Figure 9, compound **4d** stimulates ROS accumulation (86.22 Pg/ml) in RPMI-8226 cells slightly higher than gefitinib (80.29 Pg/ml) and 3 folds higher than the control cells. The results indicate that ROS accumulation can be considered as one of the major cause of apoptosis caused by compound **4d**.

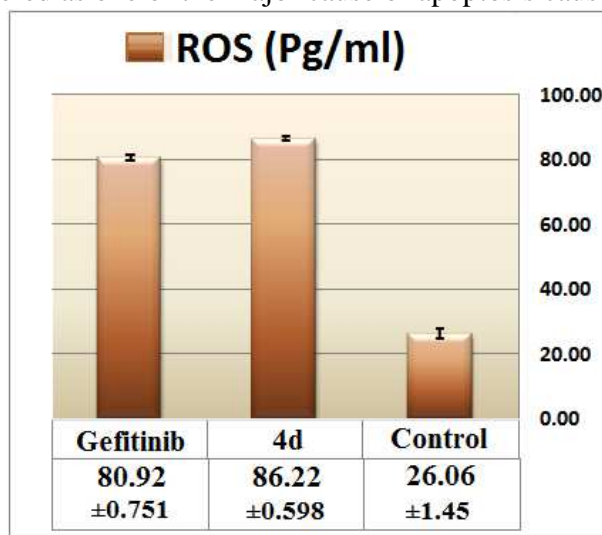


Figure 9. Effect of **4d** and gefitinib on intracellular ROS accumulation in RPMI-8226 cells.

In order to confirm the correlation between **4d**-induced apoptosis and intracellular ROS accumulation in RPMI-8226 cells, we performed cell cycle analysis of RPMI-8226 cells treated with different concentration of compound **4d** (0.6, 3 and 6 μ M) for 24 h, then ROS scavenger *N*-acetylcysteine (NAC) was added to the **4d** set (6 μ M) and its effect on the apoptosis rate was examined. The cell cycle analysis (Figure 10) showed that **4d** induced apoptosis *via* aggregation of MM RPMI-8226 cells in G2/M phase in a dose-dependent manner, where the aggregation percentage increased from 10.32% in the control cells to 19.47%, 44.18% and 49.01% in 0.6, 3 and 6 μ M **4d**-treated cells, respectively, leading to apoptosis by 15.32%, 27.56% and 34.69%, respectively. However, the aggregation of RPMI-8226 cells in G2/M phase reduced significantly from 49.01% in 6 μ M **4d**-treated cells to 33.52% after addition of NAC, leading to significant reduction in apoptosis from 34.69% to 14.89% (Figures 10 and 11). The Annexin V-fluorescein isothiocyanate/propidium iodide (Annexin V-FITC/PI) double staining (Figures 12 and 13) showed that the apoptotic rate in the late apoptotic quadrant Q2 decreased from 21.74% in 6 μ M **4d**-treated cells to 2.5% after addition of NAC. From the above investigations, it is obvious that the principal mechanism in the **4d**-induced cell death is the apoptosis induction which is initiated mainly by ROS accumulation in RPMI-8226 cells treated with **4d**.

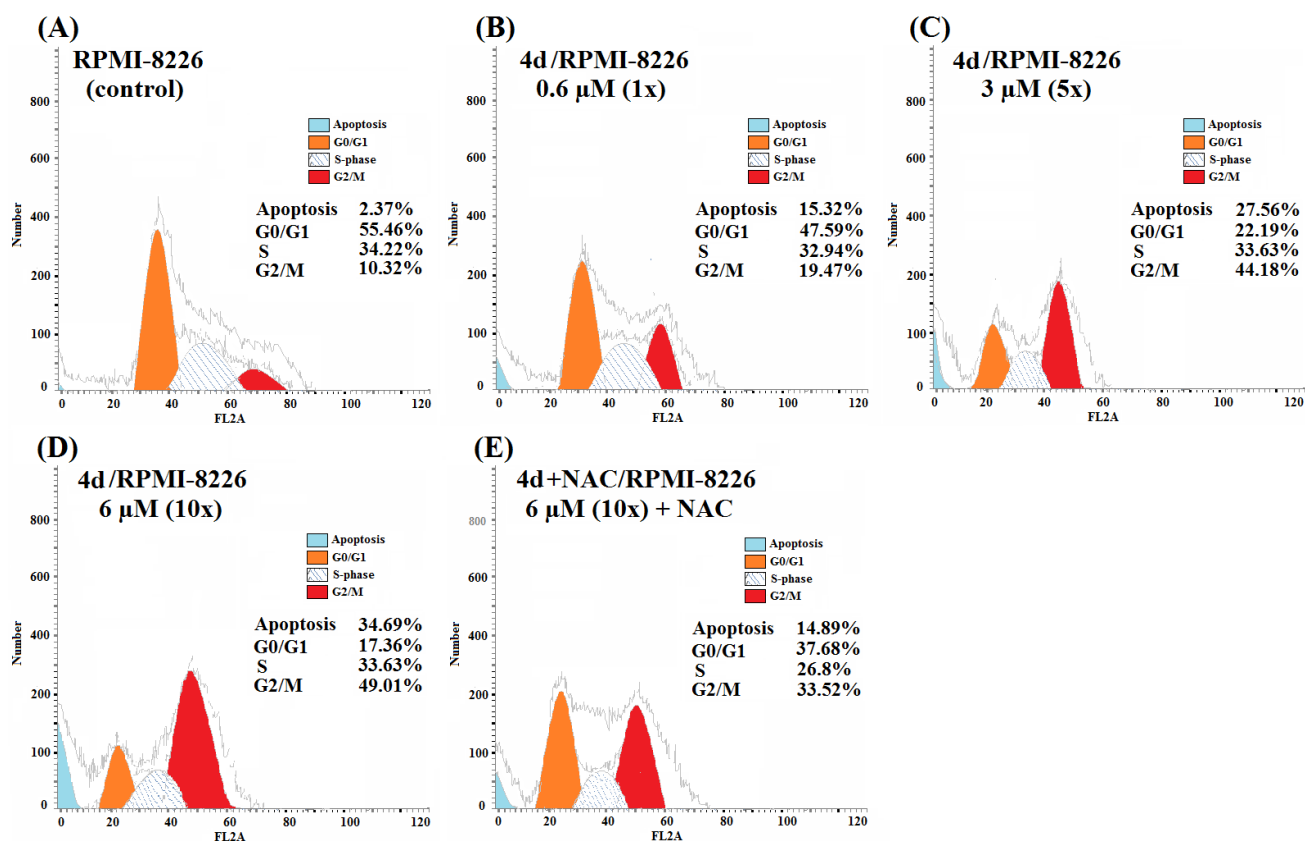


Figure 10. Flow cytometry analysis of cell cycle phase distribution in RPMI-8226 cells after treatment with different concentration of **4d** for 24 h as well as after addition of NAC. Histogram (A-E) represents propidium iodide staining of RPMI-8226 cells treated with vehicle control (DMSO) (A), compound **4d** (0.6, 3 and 6 μ M) (B-D) or compound **4d** (6 μ M) in presence of NAC (E).

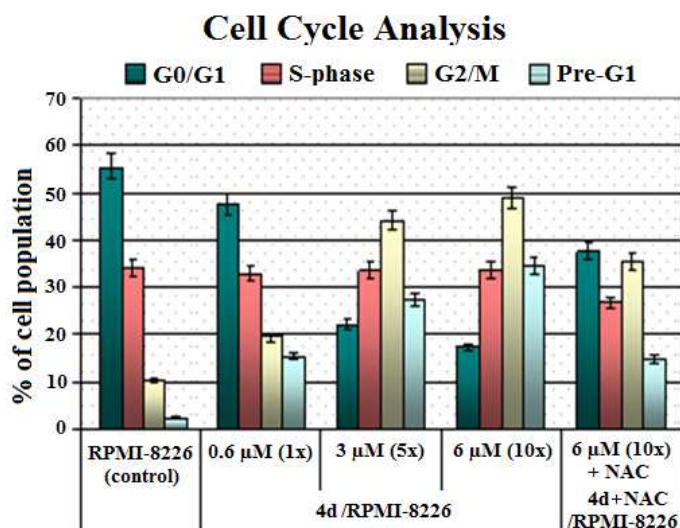


Figure 11. Bar diagram shows the cell distribution in the subG1, G0/G1, S and G2/M phases for RPMI-8226 cells treated with vehicle control and **4d** (0.6, 3 and 6 μ M with or without NAC). NAC: *N*-acetylcysteine.

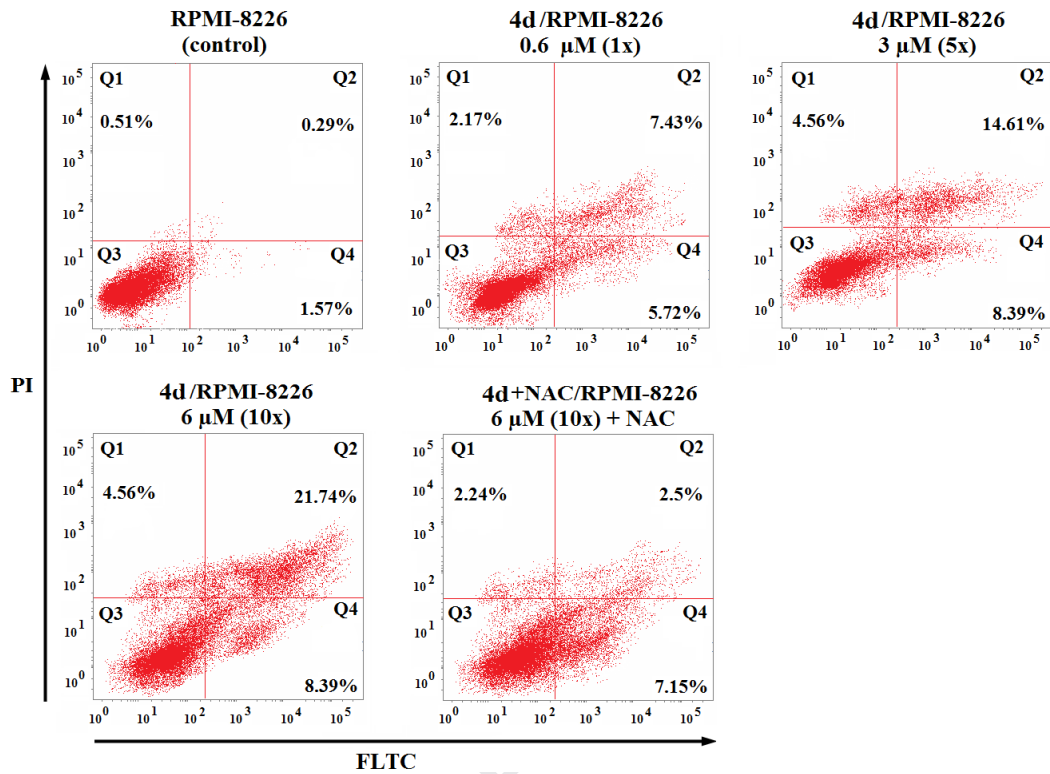


Figure 12. Annexin V-FITC/PI double staining for detection of apoptosis in RPMI-8226 cell after treatment with different concentration of **4d** for 24 h as well as after addition of NAC. Q4 quadrant represent early apoptosis; Q2 quadrant represent late apoptosis; Q1 quadrant represent dead (necrotic) cells; Q3 quadrant represent live cells. Summation of early and late apoptosis represents total apoptosis.

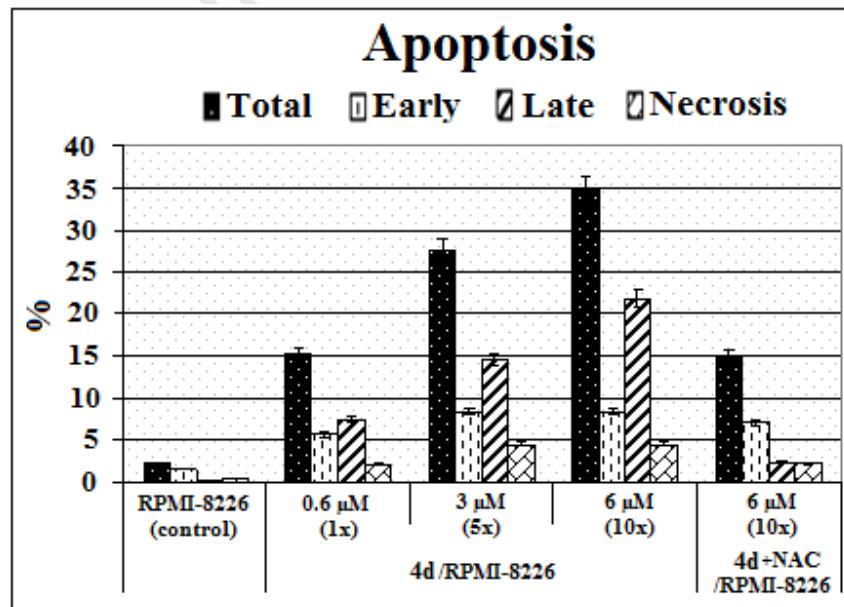


Figure 13. Bar diagram shows % apoptosis in RPMI-8226 cells treated with vehicle control and **4d** (0.6, 3 and 6 μ M with or without NAC). NAC: *N*-acetylcysteine. Summation of early and late apoptosis represents total apoptosis.

From the previous mechanistic evaluation, we can conclude that triazole-chalcone **4d** exerts its anticancer effect through induction of apoptosis in MM RPMI-8226 cells, which caused by triggering mitochondrial apoptotic pathway. This apoptotic pathway is initiated by ROS accumulation, increasing Bax/Bcl-2 ratio and activation of caspases 3, 7 and 9.

3. Conclusion

New hybrids of 1,2,3-triazole-chalcone were synthesized and evaluated for their antiproliferative activities against a panel of NCI-60 cancer cell lines. Compound **4d** having 3,4-dimethoxyphenyl moiety was the most potent anticancer agent with broad spectrum activity against RPMI-8226 leukemia, SR leukemia, K-562 leukemia, M14 melanoma, MCF7 breast, HCT-116 colon and PC-3 prostate cancer cell lines. Mechanistic evaluation of hybride **4d** in RPMI-8226 cells was studied through measuring its effect on HDACs, NF- κ B, EGFR, VEGFR, topoisomerase 2, tubulin, Bax, Bcl-2, caspases 3, 7, 9 and PARP-1. Compound **4d** causes cell cycle arrest at G2/M phase and induced apoptosis in a dose dependant manner *via* triggering mitochondrial apoptotic pathway through inducing ROS accumulation, increasing Bax/Bcl-2 ratio and activation of caspases 3, 7 and 9. The current study evidently identified the potential of compound **4d** to be a promising lead for future development of active anticancer agents, and may offer new insights in treating multiple myeloma RPMI-8226.

4. Experimental

4.1. General

Melting points were determined on Stuart melting point apparatus and were uncorrected. IR spectra were recorded on Thermo Fisher SCIENTIFIC Nicolet IS10 Spectrometer (ν in cm^{-1}). Mass spectrometry (EI) m/z analyses were performed using Hewlett Packard 5988 spectrometer. The ^1H and ^{13}C NMR spectra were recorded on a Joel 500 MHz spectrometer, ^1H spectra were run at 500 MHz and ^{13}C spectra were run at 125 MHz in deuterated dimethylsulphoxide (DMSO-d_6), chemical shifts are quoted in δ as parts per million (ppm) using solvent peak as standard. TLC was carried out using Kieselgel 60 F254 sheets (Merck, Darmstadt, Germany), the developing solvents were ethyl acetate/petroleum ether (3:1) or dichloromethane/methanol (20:1) and the spots were visualized using UV lamp at 366 or 254 nm. Compounds **1a** and **1b** were purchased, while compounds **2a**, **2b** [33], **3a** and **3b** [34] were prepared according to the reported procedures.

4.2. General procedure for synthesis of compounds **4a-k**

To a suspension of compound **3** (0.01 mol) in EtOH (95%, 20 ml), substituted aldehyde (0.01 mol) was added and stirred in an ice bath. A solution of NaOH (6 gm) in EtOH (95%, 30 ml) was added to the mixture dropwise with continuous stirring for 30 min. The reaction mixture was stirred at room temperature for 24–72 hours, the completion of the reaction was judged by TLC. After that it was diluted with ice-cold water (40 ml) and neutralized with HCl solution. The separated solids were filtered, washed with cold water and dried to give the titled compound **4a-k** without further purification.

4.2.1. (E)-1-[1-(4-Chlorophenyl)-5-methyl-triazol-4-yl]-3-[4-(dimethylamino)phenyl]prop-2-en-1-one (**4a**)

Orange solid; Yield = 72%; m.p. = 192-195 °C; ¹H NMR (500 MHz, DMSO-d₆): δ = 7.78 (d, *J* = 15.9 Hz, 1H), 7.75 (d, *J* = 15.9 Hz, 1H), 7.75 (d, *J* = 9.0 Hz, 2H), 7.72 (d, *J* = 9.0 Hz, 2H), 7.66 (d, *J* = 8.9 Hz, 2H), 6.77 (d, *J* = 8.9 Hz, 2H), 3.02 (s, 6H), 2.59 (s, 3H); ¹³C NMR (125 MHz, DMSO-d₆): δ = 183.3, 152.5, 144.6, 143.7, 138.8, 135.1, 134.3, 131 (2C), 130.1 (2C), 127.6 (2C), 121.9, 117.1, 112.2 (2C), 39.5 (2C), 10.2; MS (EI) *m/z* (Chemical Formula: C₂₀H₁₉ClN₄O): 366.9 (56.26%) [M⁺]; IR (KBr, cm⁻¹): 3447, 3101, 2909, 2813, 1653 (C=O α,β-unsaturated), 1568, 1528, 1498, 1431, 1366, 1181, 1033, 997, 825.

4.2.2. (E)-1-[1-(4-Chlorophenyl)-5-methyl-triazol-4-yl]-3-(4-fluorophenyl)prop-2-en-1-one (**4b**)

Pale yellow solid; Yield = 65%; m.p. = 195-197 °C; ¹H NMR (500 MHz, DMSO-d₆): δ = 7.99 (d, *J* = 16.0 Hz, 1H), 7.94 (dd, *J* = 8.6, 5.7 Hz, 2H), 7.87 (d, *J* = 16.0 Hz, 1H), 7.76 (d, *J* = 9.0 Hz, 2H), 7.73 (d, *J* = 9.0 Hz, 2H), 7.32 (t, *J* = 8.8 Hz, 2H), 2.61 (s, 3H); ¹³C NMR (125 MHz, DMSO-d₆): δ = 183.8, 164 (d, ¹JCF = 249.4 Hz), 143.6, 142.6, 139.8, 135.4, 134.4, 131.7 (d, ³JCF = 8.8 Hz, 2C), 131.5 (d, ⁴JCF = 2.4 Hz), 130.3 (2C), 127.8 (2C), 123, 116.7 (d, ²JCF = 21.8 Hz, 2C), 10.4; MS (EI) *m/z* (Chemical Formula: C₁₈H₁₃ClFN₃O): 342.01 (26.58%) [M⁺]; IR (KBr, cm⁻¹): 3449, 3073, 1667 (C=O α,β-unsaturated), 1590, 1498, 1422, 1363, 1227, 1187, 1159, 1028, 999, 977, 833.

4.2.3. (E)-1-[1-(4-Chlorophenyl)-5-methyl-triazol-4-yl]-3-(2-furyl)prop-2-en-1-one (**4c**)

Pale yellow solid; Yield = 60%; m.p. = 146-148 °C; ¹H NMR (500 MHz, DMSO-d₆): δ = 7.95 (d, *J* = 1.0 Hz, 1H), 7.76 (d, *J* = 15.8 Hz, 1H), 7.75 (d, *J* = 9.0 Hz, 2H), 7.73 (d, *J* = 9.0 Hz, 2H), 7.67 (d, *J* = 15.8 Hz, 2H), 7.13 (d, *J* = 3.4 Hz, 1H), 6.71 (dd, *J* = 3.4, 1.8 Hz, 1H), 2.60 (s, 3H); ¹³C NMR (125 MHz, DMSO-d₆): δ = 183.2, 151.3, 146.9, 143.4, 139.5, 135.2, 134.2, 130.2 (2C), 129.8, 127.7 (2C), 119.8, 118.1, 113.6, 10.2; MS (EI) *m/z* (Chemical Formula: C₁₆H₁₂ClN₃O₂): 313.98 (14.39%) [M⁺]; IR (KBr, cm⁻¹): 3424, 3098, 3059, 1660 (C=O α,β-unsaturated), 1600, 1557, 1501, 1424, 1363, 1269, 1211, 1032, 996, 836, 753.

4.2.4. (E)-1-[1-(4-Chlorophenyl)-5-methyl-triazol-4-yl]-3-(3,4-dimethoxyphenyl)prop-2-en-1-one (**4d**)

Yellow solid; Yield = 61%; m.p. = 166-168 °C; ¹H NMR (500 MHz, DMSO-d₆): δ = 7.91 (d, *J* = 15.9 Hz, 1H), 7.82 (d, *J* = 15.9 Hz, 1H), 7.75 (d, *J* = 9.0 Hz, 2H), 7.73 (d, *J* = 9.0 Hz, 2H), 7.44 (d, *J* = 1.7 Hz, 1H), 7.40 (dd, *J* = 8.4, 1.7 Hz, 1H), 7.05 (d, *J* = 8.4 Hz, 1H), 3.87 (s, 3H), 3.83 (s, 3H), 2.61 (s, 3H); ¹³C NMR (125 MHz, DMSO-d₆): δ = 183.7, 151.8, 149.4, 144.1, 143.6, 139.4, 135.2, 134.3, 130.2 (2C), 127.7 (2C), 127.6, 124, 120.8, 112.1, 111, 56 (2C), 10.3; MS (EI) *m/z* (Chemical Formula: C₂₀H₁₈ClN₃O₃): 384.04 (21.87%) [M⁺]; IR (KBr, cm⁻¹): 3447, 3070, 2997, 2968, 2936, 2836, 1658 (C=O α,β-unsaturated), 1581, 1509, 1424, 1339, 1257, 1134, 1028, 996, 980, 840.

4.2.5. (E)-1-[1-(4-Chlorophenyl)-5-methyl-triazol-4-yl]-3-(3-hydroxy-4-methoxy-phenyl)prop-2-en-1-one (**4e**)

Brown solid; Yield = 70%; m.p. = 236-239 °C; ¹H NMR (500 MHz, DMSO-d₆): δ = 9.36 (s, 1H), 7.79 (d, *J* = 15.8 Hz, 1H), 7.76 (d, *J* = 15.8 Hz, 1H), 7.75 (d, *J* = 8.9 Hz, 2H), 7.73 (d, *J* = 8.9 Hz, 2H), 7.26 (d, *J* = 1.7 Hz, 1H), 7.24 (dd, *J* = 8.2, 1.7 Hz, 1H), 7.01 (d, *J* = 8.2 Hz, 1H), 3.83 (s, 3H), 2.59 (s, 3H); ¹³C NMR (125 MHz, DMSO-d₆): δ = 183.1, 150.6, 146.9, 143.6, 143.2, 138.9, 134.8, 133.9, 129.8 (2C), 127.3 (2C), 127.2, 122.3, 119.9, 114, 112.1, 55.6, 9.7; MS (EI) *m/z* (Chemical Formula: C₁₉H₁₆ClN₃O₃): 369.31 (100%) [M⁺]; IR (KBr, cm⁻¹): 3351, 3011, 2957, 2930, 2839, 1657 (C=O α,β-unsaturated), 1588, 1550, 1505, 1439, 1271, 1034, 984, 830.

4.2.6. (*E*)-1-[1-(4-Chlorophenyl)-5-methyl-triazol-4-yl]-3-(4-hydroxy-3-methoxy-phenyl)prop-2-en-1-one (**4f**)

Yellow solid; Yield = 59%; m.p. = 164 -167 °C; ¹H NMR (500 MHz, DMSO-d₆): δ = 9.82 (s, 1H), 7.85 (d, *J* = 15.8 Hz, 1H), 7.79 (d, *J* = 15.8 Hz, 1H), 7.75 (d, *J* = 9.0 Hz, 2H), 7.73 (d, *J* = 9.0 Hz, 2H), 7.41 (d, *J* = 1.7 Hz, 1H), 7.27 (dd, *J* = 8.1, 1.7 Hz, 1H), 6.87 (d, *J* = 8.1 Hz, 1H), 3.87 (s, 3H), 2.60 (s, 3H); ¹³C NMR (125 MHz, DMSO-d₆): δ = 183.3, 150.1, 148.1, 144.2, 143.2, 138.9, 134.8, 133.9, 129.8 (2C), 127.3 (2C), 125.8, 123.9, 119.4, 115.8, 111.6, 55.7, 9.9; MS (EI) *m/z* (Chemical Formula: C₁₉H₁₆ClN₃O₃): 369.21 (100%) [M⁺]; IR (KBr, cm⁻¹): 3434, 3063, 2977, 2942, 1662 (C=O *α,β*-unsaturated), 1581, 1507, 1426, 1263, 1209, 1029, 991, 830.

4.2.7. (*E*)-3-[4-(Dimethylamino)phenyl]-1-[5-methyl-1-(4-nitrophenyl)triazol-4-yl]prop-2-en-1-one (**4g**)
Orange solid; Yield = 92%; m.p. = 247-249 °C; ¹H NMR (500 MHz, DMSO-d₆): δ = 8.50 (d, *J* = 9.0 Hz, 2H), 8.02 (d, *J* = 9.0 Hz, 2H), 7.80 (d, *J* = 15.8 Hz, 1H), 7.76 (d, *J* = 15.8 Hz, 1H), 7.67 (d, *J* = 8.9 Hz, 2H), 6.78 (d, *J* = 8.9 Hz, 2H), 3.03 (s, 6H), 2.68 (s, 3H); ¹³C NMR (125 MHz, DMSO-d₆): δ = 183.6, 153.4, 147.7, 144.8, 144, 140.3, 139.1, 130.9 (2C), 126.9 (2C), 125.7 (2C), 121.6, 117.1, 112.3 (2C), 39.5 (2C), 10.4; MS (EI) *m/z* (Chemical Formula: C₂₀H₁₉N₅O₃): 377.12 (100%) [M⁺]; IR (KBr, cm⁻¹): 3424, 3093, 2910, 1651 (C=O *α,β*-unsaturated), 1597, 1567, 1525 (NO₂), 1433, 1366, 1344 (NO₂), 1177, 1033, 996, 856.

4.2.8. (*E*)-3-(4-Fluorophenyl)-1-[5-methyl-1-(4-nitrophenyl)triazol-4-yl]prop-2-en-1-one (**4h**)

Pale yellow solid; Yield = 62%; m.p. = 196-199 °C; ¹H NMR (500 MHz, DMSO-d₆): δ = 8.51 (d, *J* = 9.0 Hz, 2H), 8.03 (d, *J* = 9.0 Hz, 2H), 8.00 (d, *J* = 16.0 Hz, 1H), 7.96 (dd, *J* = 8.7, 5.6 Hz, 2H), 7.89 (d, *J* = 16.0 Hz, 1H), 7.33 (t, *J* = 8.8 Hz, 2H), 2.69 (s, 3H); ¹³C NMR (125 MHz, DMSO-d₆): δ = 183.7, 164 (d, ¹JCF = 249.4 Hz), 148.3, 143.7, 142.7, 140.2, 140, 131.6 (d, ³JCF = 8.6 Hz, 2C), 131.4 (d, ⁴JCF = 2.8 Hz), 127 (2C), 125.5 (2C), 122.9, 116.6 (d, ²JCF = 21.7 Hz, 2C), 10.4; MS (EI) *m/z* (Chemical Formula: C₁₈H₁₃FN₄O₃): 352 (100%) [M⁺]; IR (KBr, cm⁻¹): 3447, 3093, 1666 (C=O *α,β*-unsaturated), 1595, 1522 (NO₂), 1426, 1343 (NO₂), 1231, 1031, 997, 977, 858, 832.

4.2.9. (*E*)-3-(2-Furyl)-1-[5-methyl-1-(4-nitrophenyl)triazol-4-yl]prop-2-en-1-one (**4i**)

Pale yellow solid; Yield = 92%; m.p. = 232-234 °C; ¹H NMR (500 MHz, DMSO-d₆): δ = 8.51 (d, *J* = 9.0 Hz, 2H), 8.02 (d, *J* = 9.0 Hz, 2H), 7.97 (d, *J* = 1.4 Hz, 1H), 7.78 (d, *J* = 15.7 Hz, 1H), 7.69 (d, *J* = 15.7 Hz, 1H), 7.15 (d, *J* = 3.4 Hz, 1H), 6.73 (dd, *J* = 3.4, 1.7 Hz, 1H), 2.68 (s, 3H); ¹³C NMR (125 MHz, DMSO-d₆): δ = 183.3, 151.4, 147.1, 143.8, 140.3, 139.9, 130.2, 127.1 (2C), 126.8, 125.6 (2C), 119.9, 118.4, 113.8, 10.5; MS (EI) *m/z* (Chemical Formula: C₁₆H₁₂N₄O₄): 324.05 (100%) [M⁺]; IR (KBr, cm⁻¹): 3448, 3084, 1659 (C=O *α,β*-unsaturated), 1596, 1556, 1530 (NO₂), 1502, 1425, 1347 (NO₂), 1285, 981, 860, 756.

4.2.10. (*E*)-3-(3,4-Dimethoxyphenyl)-1-[5-methyl-1-(4-nitrophenyl)triazol-4-yl]prop-2-en-1-one (**4j**)

Yellow solid; Yield = 91%; m.p. = 223-225 °C; ¹H NMR (500 MHz, DMSO-d₆): δ = 8.51 (d, *J* = 9.0 Hz, 2H), 8.02 (d, *J* = 9.0 Hz, 2H), 7.92 (d, *J* = 15.9 Hz, 1H), 7.84 (d, *J* = 15.9 Hz, 1H), 7.45 (d, *J* = 1.8 Hz, 1H), 7.41 (dd, *J* = 8.4, 1.8 Hz, 1H), 7.06 (d, *J* = 8.4 Hz, 1H), 3.87 (s, 3H), 3.83 (s, 3H), 2.68 (s, 3H); ¹³C NMR (125 MHz, DMSO-d₆): δ = 183.1, 151.4, 149.1, 147.8, 143.6, 143.3, 139.7, 138.9, 127.1, 126.3 (2C), 124.8 (2C), 123.2, 120.5, 111.9, 111.1, 55.5 (2C), 9.7; MS (EI) *m/z* (Chemical Formula:

C₂₀H₁₈N₄O₅): 394.10 (52.36%) [M⁺]; IR (KBr, cm⁻¹): 3448, 3088, 2994, 2838, 1658 (C=O α,β -unsaturated), 1587, 1521 (NO₂), 1424, 1344 (NO₂), 1263, 1239, 1139, 1033, 981, 856.

4.2.11. (*E*)-3-(3-Hydroxy-4-methoxy-phenyl)-1-[5-methyl-1-(4-nitrophenyl)triazol-4-yl]prop-2-en-1-one (**4k**)

Yellow solid; Yield = 46%; m.p. = 268-272 °C; ¹H NMR (500 MHz, DMSO-d₆): δ = 9.38 (s, 1H), 8.49 (d, *J* = 9.0 Hz, 2H), 8.01 (d, *J* = 9.0 Hz, 2H), 7.80 (d, *J* = 15.8 Hz, 1H), 7.74 (d, *J* = 15.8 Hz, 1H), 7.27 (d, *J* = 1.8 Hz, 1H), 7.24 (dd, *J* = 8.2, 1.8 Hz, 1H), 7.01 (d, *J* = 8.2 Hz, 1H), 3.83 (s, 3H), 2.67 (s, 3H); ¹³C NMR (125 MHz, DMSO-d₆): δ = 182.8, 150.3, 147.6, 146.6, 143.5, 143.1, 139.6, 138.9, 126.8, 126.3 (2C), 124.8 (2C), 122.1, 119.5, 113.7, 111.8, 55.3, 9.7; MS (EI) *m/z* (Chemical Formula: C₁₉H₁₆N₄O₅): 380.34 (100%) [M⁺]; IR (KBr, cm⁻¹): 3380, 3089, 2939, 2839, 1659 (C=O α,β -unsaturated), 1586, 1524 (NO₂), 1504, 1432, 1343 (NO₂), 1268, 1031, 980, 855.

4.3. Biological evaluation

4.3.1. Cancer cell line screening at NCI

The synthesized compounds were screened against a panel of 60 cancer cell lines derived from nine tumor types at the National Cancer Institute (NCI), Bethesda, Maryland, USA, applying the standard NCI protocol reported elsewhere [53]. The compounds were tested at a single dose concentration of 10 μ M, and the one-dose data were reported as a mean graph of the percent growth of the treated cells. The number reported for the one-dose assay is growth relative to the no-drug control, and relative to the time zero number of cells. Using the seven absorbance measurements [time zero, (Tz), control growth, (C), and test growth in the presence of drug at the five concentration levels (Ti)], the percent growth is calculated at each of the drug concentrations levels. Percent growth inhibition is calculated as:

- $[(Ti - Tz)/(C - Tz)] \times 100$ for concentrations for which $Ti \geq Tz$
- $[(Ti - Tz)/Tz] \times 100$ for concentrations for which $Ti < Tz$.

4.3.2. Cytotoxicity MTT assay for compounds **4b**, **4d**, **4f**, **4h** and **4i**

Cancer cell lines (RPMI-8226, SR, K-562, M14, MCF7, HCT-116 and PC-3) and normal cell lines (PCS-800-011, WS1, MCF 10A, CCD-18Co and HPrEC) were used to verify the cytotoxicity of compounds **4b**, **4d**, **4f**, **4h** and **4i** using the MTT assay. The principle of this assay is the transformation of the yellow tetrazolium bromide (MTT) to a purple formazan derivative by mitochondrial succinate dehydrogenase in viable cells [54]. Cell lines were cultured in RPMI-1640 medium with 10% fetal bovine serum. The antibiotics added were 100 μ g/ml streptomycin and 100 units/ml penicillin at 37° C in a 5% CO₂ incubator. The cell lines were planted in a 96-well plate at a density of 1.0×10^4 cells/ well at 37° C for 48 h under 5% CO₂ [55]. After incubation, the cells were handled with several concentrations of the synthesized compounds and incubated for 24 h. After that, 20 μ l of MTT solution at 5 mg/ml was included and incubated for 4 h. Dimethyl sulfoxide (DMSO) in volume of 100 μ l is supplemented into each well to dissolve the purple formazan made. The absorbance was measured at a wavelength of 570 nm using a plate reader (EXL 800 USA), and IC₅₀ values were determined.

4.3.3. *In vitro* enzyme inhibitory assays (against HDAC, NF- κ B, EGFR, VEGFR-2, topoisomerase-2 and tubulin) as well as intracellular ROS accumulation assay of compound **4d** in RPMI-8226 cell line

In vitro enzyme inhibitory assay of compound **4d** was performed against five HDAC isoforms (HDAC1, 2, 3, 8, 6) using ELISA assay kits (Mybiosource, Inc.), NF- κ B using ELISA assay kits (ab176648–NF κ B p65 Total Simple Step ELISA™ Kit), EGFR using ELISA kit for EGFR (cloud clone SEA757Hu 96 Tests), VEGFR-2 using ELISA kit for VEGFR-2 (RayBio_Human VEGFR2), topoisomerase-2 using ELISA kit for TOP2B (human DNA topoisomerase 2-beta, MBS942146) and tubulin using ELISA kit for TUBb (Cloud-Clone Corp., SEB870Hu 96 Tests Enzyme-linked Immunosorbent Assay Kit) as well as intracellular ROS accumulation assay using ELISA kit for ROS (EIAab ROS eia kit). The procedure of the used kit was done according to the manufacturer's instructions. Briefly, 96-well microtiter plates were used for RPMI-8226 growing cells in which trypsinization, counting and seeding of cells at the proper densities were carried out followed by incubation at 37 °C in a humidified atmosphere for 24 h. The standards, **4d** compound, and the positive reference (Velcade as HDAC inhibitor; Gefitinib as NF- κ B and EGFR inhibitor; Sorafenib as VEGFR-2 inhibitor; Doxorubicin as topoisomerase-2 inhibitor; Combretastatin as tubulin inhibitor; Gefitinib as ROS generator) were adjusted to nominated concentrations. Then 100 μ L of sample or standard was added to each well of the 96-well microtiter plates, and incubated for 2 h at 37 °C. After aspiration of the solution, prepared Detection Reagent A was added in 100 μ L to each well and incubated for 1 h at 37 °C. Washing was performed, then prepared Detection Reagent B was added in 100 μ L, and incubation was continued for another 1 h at 37 °C. Afterthat, Five washings were performed followed by addition of 3,3',5,5'-tetramethylbenzidine (TMB) substrate solution in 90 μ L and incubation for 15–25 min at 37 °C. Next, Stop solution was added in 50 μ L. Cells were exposed to different concentrations of compound **4d** and reference for 72 h. Optical density (O.D.) was measured at 450 nm using microplate reader. The values of % activity versus a series of compound concentrations (with semi-log decrease in concentration) were then plotted using non-linear regression analysis of sigmoidal dose-response curve, and the concentration that induces 50% of maximum inhibition (IC₅₀) of HDAC isoforms, NF- κ B, EGFR, VEGFR-2, topoisomerase-2 and tubulin were determined.

4.3.4. *Measurement of the effect of compound 4d on the level of BAX, Bcl-2, caspases 3, 7, 9 and PARP-1 in RPMI-8226 cell line*

The level of BAX (apoptotic marker), Bcl-2 (anti-apoptotic marker), caspases 3, 7, 9 and PARP-1 (apoptotic markers) were assessed using ELISA colorimetric kits (ELISA kit for BAX (DRG® Human, EIA-4487), ELISA kit for Bcl-2 (Invitrogen Zymed®), ELISA kit for caspases (Invetrogen Casp3, Casp7, Casp9 (Active) eia kit) and ELISA kit for PARP-1 (Abcam PARP-1 Human eia kit ab110215)). The procedure of the used kit was done according to the manufacturer's instructions. Briefly, RPMI-8226 Cells (obtained from American Type Culture Collection) were grown in RPMI 1640 containing 10% fetal bovine serum at 37°C. Cells were Plated in a density of 1.2–1.8 \times 10,000 cells/well in a volume of 100 μ l complete growth medium + 100 μ l of the compound **4d** per well in a 96-well plate for 24 hours before the assay and lysed with Cell Extraction Buffer. This lysate was diluted in Standard Diluent Buffer over the range of the assay and measured for human active BAX, Bcl-2, caspase-3, caspase-7, caspase-9 or PARP-1 content.

4.3.5. *Cell cycle analysis of compound 4d in RPMI-8226 cells*

The RPMI-8226 cells were treated with compound **4d** at three concentrations (IC_{50} (x), 5x and 10x) in absence of NAC, and at concentration 10x of compound **4d** in presence of NAC for 24 h. After treatment, the cells were washed twice with ice-cold phosphate buffer saline (PBS), collected by centrifugation, and fixed in ice-cold 70% (v/v) ethanol, washed with PBS, re-suspended with 0.1 mg/mL RNase, stained with 40 mg/mL propidium iodide (PI), and analyzed by flow cytometry using FACSCalibur (Becton Dickinson) [56]. The cell cycle distributions were calculated using Cell-Quest software (Becton Dickinson).

4.3.6. Annexin-V-FITC apoptosis assay of compound **4d** in RPMI-8226 cells

Apoptosis was determined by staining the cells with Annexin V fluorescein isothiocyanate (FITC) and counterstaining with PI using the Annexin V-FITC/PI apoptosis detection kit (BD Biosciences, San Diego, CA) according to the manufacturer's instructions. Briefly, 4×10^6 cell/T 75 flask were exposed to compounds **4d** at three concentrations (IC_{50} (x), 5x and 10x) in absence of NAC, and at concentration 10x of compound **4d** in presence of NAC for 24 h. The cells then were collected by trypsinization and 0.5×10^6 cells were washed twice with PBS and stained with 5 μ L Annexin V-FITC and 5 μ L PI in 1 \times binding buffer for 15 min at room temperature in the dark. Analyses were performed using FACS Calibur flow cytometer (BD Biosciences, San Jose, CA).

4.4. Statistical analysis

In this study part of the data is presented as mean \pm SD of three individual experiments performed in triplicate. Non-parametric one-way analysis of variance (ANOVA) followed by a Dunnett post-hoc test was applied for Statistical analysis using the SPSS software (version 18.0). $P < 0.05$ was regarded statistically significant.

Acknowledgments

Our sincere thanks to the National Cancer Institute (NCI), USA, for carrying out the *in vitro* antiproliferative analysis.

References

- [1] A. Jemal, F. Bray, M.M. Center, J. Ferlay, E. Ward, D. Forman, Global cancer statistics, *CA-Cancer J. Clin.* 61 (2011) 69-90.
- [2] (a) J.E. Noll, S.A. Williams, C.M. Tong, H. Wang, J.M. Quach, L.E. Purton, K. Pilkington, L.B. To, A. Evdokiou, S. Gronthos, Myeloma plasma cells alter the bone marrow microenvironment by stimulating the proliferation of mesenchymal stromal cells, *Haematologica.* 99 (2014) 163-171; (b) S.V. Rajkumar, Multiple myeloma, *Curr. Probl. Cancer.* 33 (2009) 7-64.
- [3] (a) S.V. Rajkumar, S. Kumar, Multiple myeloma: diagnosis and treatment, in: *Mayo Clinic Proceedings*, Elsevier, 2016, pp. 101-119; (b) I. Vaxman, M.H. Sidiqi, M. Gertz, Venetoclax for the treatment of multiple myeloma, *Expert review of hematology*, 11 (2018) 915-920; (c) C. Chen, D. Siegel, M. Gutierrez, M. Jacoby, C.C. Hofmeister, N. Gabrail, R. Baz, M. Mau-Sorensen, J.G. Berdeja, M. Savona, Safety and efficacy of selinexor in relapsed or refractory multiple myeloma and Waldenstrom macroglobulinemia, *Blood*, 131 (2018) 855-863.
- [4] S. Deleu, M. Lemaire, J. Arts, E. Menu, E. Van Valckenborgh, P. King, I.V. Broeck, H. De Raeve, B. Van Camp, P. Croucher, The effects of JNJ-26481585, a novel hydroxamate-based histone deacetylase

- inhibitor, on the development of multiple myeloma in the 5T2MM and 5T33MM murine models, *Leukemia*, 23 (2009) 1894-1903.
- [5] J. Kikuchi, T. Wada, R. Shimizu, T. Izumi, M. Akutsu, K. Mitsunaga, K. Noborio-Hatano, M. Nobuyoshi, K. Ozawa, Y. Kano, Histone deacetylases are critical targets of bortezomib-induced cytotoxicity in multiple myeloma, *Blood*, 116 (2010) 406-417.
- [6] B. Cao, J. Li, J. Zhu, M. Shen, K. Han, Z. Zhang, Y. Yu, Y. Wang, D. Wu, S. Chen, The antiparasitic clioquinol induces apoptosis in leukemia and myeloma cells by inhibiting histone deacetylase activity, *J. Biol. Chem.* 288 (2013) 34181-34189.
- [7] T. Hideshima, J. Qi, R.M. Paranal, W. Tang, E. Greenberg, N. West, M.E. Colling, G. Estiu, R. Mazitschek, J.A. Perry, Discovery of selective small-molecule HDAC6 inhibitor for overcoming proteasome inhibitor resistance in multiple myeloma, *Proc. Natl. Acad. Sci.* 113 (2016) 13162-13167.
- [8] C.M. Annunziata, R.E. Davis, Y. Demchenko, W. Bellamy, A. Gabrea, F. Zhan, G. Lenz, I. Hanamura, G. Wright, W. Xiao, Frequent engagement of the classical and alternative NF- κ B pathways by diverse genetic abnormalities in multiple myeloma, *Cancer cell*. 12 (2007) 115-130.
- [9] J.J. Keats, R. Fonseca, M. Chesi, R. Schop, A. Baker, W.-J. Chng, S. Van Wier, R. Tiedemann, C.-X. Shi, M. Sebag, Promiscuous mutations activate the noncanonical NF- κ B pathway in multiple myeloma, *Cancer cell*. 12 (2007) 131-144.
- [10] K. Mahtouk, M. Jourdan, J. De Vos, C. Hertogh, G. Fiol, E. Jourdan, J.-F. Rossi, B. Klein, An inhibitor of the EGF receptor family blocks myeloma cell growth factor activity of HB-EGF and potentiates dexamethasone or anti-IL-6 antibody-induced apoptosis, *Blood*. 103 (2004) 1829-1837.
- [11] J.h. Ding, L.y. Yuan, R.B. Huang, G.a. Chen, Aspirin inhibits proliferation and induces apoptosis of multiple myeloma cells through regulation of Bcl-2 and Bax and suppression of VEGF, *Eur. J. Haematol.* 93 (2014) 329-339.
- [12] G.J. Madlambayan, A.M. Meacham, K. Hosaka, S. Mir, M. Jorgensen, E.W. Scott, D.W. Siemann, C.R. Cogle, Leukemia regression by vascular disruption and antiangiogenic therapy, *Blood*. 116 (2010) 1539-1547.
- [13] Y. Zhen, B. Shang, X. Liu, Y. Lin, Y. Zhen, Antitumor efficacy of lidamycin against human multiple myeloma RPMI 8226 cells and the xenograft in nonobese diabetic/severe combined immunodeficiency mice, *J. CANCER RES. THER.* 12 (2016) 182.
- [14] L.-J. Yang, Y. Chen, J. He, S. Yi, L. Wen, S. Zhao, G.-H. Cui, Effects of gambogic acid on the activation of caspase-3 and downregulation of SIRT1 in RPMI-8226 multiple myeloma cells via the accumulation of ROS, *Oncol. Lett.* 3 (2012) 1159-1165.
- [15] (a) P. Yadav, K. Lal, A. Kumar, S.K. Guru, S. Jaglan, S. Bhushan, Green synthesis and anticancer potential of chalcone linked-1, 2, 3-triazoles, *Eur. J. Med. Chem.* 126 (2017) 944-953; (b) G. Wang, J. Qiu, X. Xiao, A. Cao, F. Zhou, Synthesis, biological evaluation and molecular docking studies of a new series of chalcones containing naphthalene moiety as anticancer agents, *Bioorg. Chem.* 76 (2018) 249-257. (c) R. Kant, D. Kumar, D. Agarwal, R.D. Gupta, R. Tilak, S.K. Awasthi, A. Agarwal, Synthesis of newer 1, 2, 3-triazole linked chalcone and flavone hybrid compounds and evaluation of their antimicrobial and cytotoxic activities, *Eur. J. Med. Chem.* 113 (2016) 34-49.
- [16] (a) D. Ušjak, B. Ivković, D.D. Božić, L. Bošković, M. Milenković, Antimicrobial activity of novel chalcones and modulation of virulence factors in hospital strains of *Acinetobacter baumannii* and *Pseudomonas aeruginosa*, *Microb. Pathogenesis*. 131 (2019) 186-196.; (b) P. Yadav, K. Lal, L. Kumar,

- A. Kumar, A. Kumar, A.K. Paul, R. Kumar, Synthesis, crystal structure and antimicrobial potential of some fluorinated chalcone-1, 2, 3-triazole conjugates, *Eur. J. Med. Chem.* 155 (2018) 263-274; (c) M. Xu, P. Wu, F. Shen, J. Ji, K. Rakesh, Chalcone derivatives and their antibacterial activities: current development, *Bioorg. Chem.* (2019) 103133.
- [17] (a) M.N. Gomes, R.C. Braga, E.M. Grzelak, B.J. Neves, E. Muratov, R. Ma, L.L. Klein, S. Cho, G.R. Oliveira, S.G. Franzblau, QSAR-driven design, synthesis and discovery of potent chalcone derivatives with antitubercular activity, *Eur. J. Med. Chem.* 137 (2017) 126-138; (b) L.F. Castaño, V. Cuartas, A. Bernal, A. Insuasty, J. Guzman, O. Vidal, V. Rubio, G. Puerto, P. Lukáč, V. Vimberg, New chalcone-sulfonamide hybrids exhibiting anticancer and antituberculosis activity, *Eur. J. Med. Chem.* 176 (2019) 50-60.
- [18] (a) S.-J. Won, C.-T. Liu, L.-T. Tsao, J.-R. Weng, H.-H. Ko, J.-P. Wang, C.-N. Lin, Synthetic chalcones as potential anti-inflammatory and cancer chemopreventive agents, *Eur. J. Med. Chem.* 40 (2005) 103-112; (b) H. ur Rashid, X. Yiming, N. Ahmad, Y. Muhammad, L. Wang, Promising anti-inflammatory effects of chalcones via inhibition of cyclooxygenase, prostaglandin E2, inducible NO synthase and nuclear factor κ B activities, *Bioorg. chem.* 87 (2019) 335-365.
- [19] (a) B. Mathew, A.A. Adeniyi, M. Joy, G.E. Mathew, A. Singh-Pillay, C. Sudarsanakumar, M.E. Soliman, J. Suresh, Anti-oxidant behavior of functionalized chalcone-a combined quantum chemical and crystallographic structural investigation, *J. Mol. Struct.* 1146 (2017) 301-308; (b) E. Polo, N. Ibarra-Arellano, L. Prent-Peñaloza, A. Morales-Bayuelo, J. Henao, A. Galdámez, M. Gutiérrez, Ultrasound-assisted synthesis of novel chalcone, heterochalcone and bis-chalcone derivatives and the evaluation of their antioxidant properties and as acetylcholinesterase inhibitors, *Bioorg. Chem.* (2019) 103034.
- [20] (a) R. Arancibia, C. Biot, G. Delaney, P. Roussel, A. Pascual, B. Pradines, A.H. Klahn, Cyrhretrenyl chalcones: Synthesis, characterization and antimalarial evaluation, *J. Organomet. Chem.* 723 (2013) 143-148; (b) R.H. Hans, E.M. Guantai, C. Lategan, P.J. Smith, B. Wan, S.G. Franzblau, J. Gut, P.J. Rosenthal, K. Chibale, Synthesis, antimalarial and antitubercular activity of acetylenic chalcones, *Bioorg. Med. Chem. Lett.* 20 (2010) 942-944.
- [21] J. Shin, M.G. Jang, J.C. Park, Y. Do Koo, J.Y. Lee, K.S. Park, S.S. Chung, K. Park, Antidiabetic effects of trihydroxychalcone derivatives via activation of AMP-activated protein kinase, *J. Ind. Eng. Chem.* 60 (2018) 177-184.
- [22] H. Kumar, V. Devaraji, R. Joshi, M. Jadhao, P. Ahirkar, R. Prasath, P. Bhavana, S.K. Ghosh, Antihypertensive activity of a quinoline appended chalcone derivative and its site specific binding interaction with a relevant target carrier protein, *RSC Adv.* 5 (2015) 65496-65513.
- [23] (a) D.K. Mahapatra, S.K. Bharti, V. Asati, Anti-cancer chalcones: Structural and molecular target perspectives, *Eur. J. Med. Chem.* 98 (2015) 69-114; (b) D. D Jandial, C. A Blair, S. Zhang, L. S Krill, Y.-B. Zhang, X. Zi, Molecular targeted approaches to cancer therapy and prevention using chalcones, *Curr. Cancer Drug Tar.* 14 (2014) 181-200.
- [24] M. Das, K. Manna, Chalcone scaffold in anticancer armamentarium: a molecular insight, *J. Toxicol.* 2016 (2016).
- [25] (a) Y.-C. Hseu, M.-S. Lee, C.-R. Wu, H.-J. Cho, K.-Y. Lin, G.-H. Lai, S.-Y. Wang, Y.-H. Kuo, K. Senthil Kumar, H.-L. Yang, The chalcone flavokawain B induces G2/M cell-cycle arrest and apoptosis in human oral carcinoma HSC-3 cells through the intracellular ROS generation and downregulation of the Akt/p38 MAPK signaling pathway, *J. Agr. Food Chem.* 60 (2012) 2385-2397; (b) C.-T. Chang, Y.-C. Hseu, V. Thiyagarajan, K.-Y. Lin, T.-D. Way, M. Korivi, J.-W. Liao, H.-L. Yang, Chalcone flavokawain B induces autophagic-cell death via reactive oxygen species-mediated signaling pathways in human gastric carcinoma and suppresses tumor growth in nude mice, *Arch. Toxicol.* 91 (2017) 3341-3364.

- [26] R. Nishimura, K. Tabata, M. Arakawa, Y. Ito, Y. Kimura, T. Akihisa, H. Nagai, A. Sakuma, H. Kohno, T. Suzuki, Isobavachalcone, a chalcone constituent of *Angelica keiskei*, induces apoptosis in neuroblastoma, *Biol. Pharm. Bull.* 30 (2007) 1878-1883.
- [27] P. Champelovier, X. Chauchet, F. Hazane-Puch, S. Vergnaud, C. Garrel, F. Laporte, J. Boutonnat, A. Boumendjel, Cellular and molecular mechanisms activating the cell death processes by chalcones: Critical structural effects, *Toxicol. In Vitro.* 27 (2013) 2305-2315.
- [28] O. Mesenzani, A. Massarotti, M. Giustiniano, T. Pirali, V. Bevilacqua, A. Caldarelli, P. Canonico, G. Sorba, E. Novellino, A.A. Genazzani, Replacement of the double bond of antitubulin chalcones with triazoles and tetrazoles: Synthesis and biological evaluation, *Bioorg. Med. Chem. Lett.* 21 (2011) 764-768.
- [29] S.U.F. Rizvi, H.L. Siddiqui, M. Nisar, N. Khan, I. Khan, Discovery and molecular docking of quinolyl-thienyl chalcones as anti-angiogenic agents targeting VEGFR-2 tyrosine kinase, *Bioorg. Med. Chem. Lett.* 22 (2012) 942-944.
- [30] D. Dheer, V. Singh, R. Shankar, Medicinal attributes of 1, 2, 3-triazoles: Current developments, *Bioorg. Chem.* 71 (2017) 30-54.
- [31] (a) S.G. Agalave, S.R. Maujan, V.S. Pore, Click chemistry: 1, 2, 3-triazoles as pharmacophores, *Chem. Asian J.* 6 (2011) 2696-2718; (b) J.K. Sahu, S. Ganguly, A. Kaushik, Triazoles: A valuable insight into recent developments and biological activities, *Chin. J. Nat. Medicines*, 11 (2013) 456-465; (c) S. Haider, M.S. Alam, H. Hamid, 1, 2, 3-Triazoles: scaffold with medicinal significance, *Inflamm Cell Signal*, 95 (2014) 1-12; (d) K. Bozorov, J. Zhao, H.A. Aisa, 1, 2, 3-Triazole-containing hybrids as leads in medicinal chemistry: A recent overview, *Bioorg. Med. Chem.* 27 (2019) 3511-3531.
- [32] (a) H. Li, R. Aneja, I. Chaiken, Click chemistry in peptide-based drug design, *Molecules*, 18 (2013) 9797-9817; (b) E. Bonandi, M.S. Christodoulou, G. Fumagalli, D. Perdicchia, G. Rastelli, D. Passarella, The 1, 2, 3-triazole ring as a bioisostere in medicinal chemistry, *Drug Discov. Today.* 22 (2017) 1572-1581.
- [33] I. Wilkening, G. del Signore, C.P. Hackenberger, Phosphoramidate peptides synthesis by Staudinger reactions of silylated phosphinic acids and esters, *Chem. Commun.* 47 (2011) 349-351.
- [34] N.T. Pokhodylo, Y.O. Teslenko, V.S. Matiychuk, M.D. Obushak, Synthesis of 2,1-Benzisoxazoles by Nucleophilic Substitution of Hydrogen in Nitroarenes Activated by the Azole Ring, *Synthesis*, 16 (2009) 2741-2748.
- [35] NCI website: <https://dtp.cancer.gov/> (retrieved on July 27th, 2019).
- [36] DTP Data Search: <http://dtp.nci.nih.gov/dtpstandard/dwindex/index.jsp>. (retrieved on July 27th, 2019).
- [37] R.B. Badisa, S.F. Darling-Reed, P. Joseph, J.S. Cooperwood, L.M. Latinwo, C.B. Goodman, Selective cytotoxic activities of two novel synthetic drugs on human breast carcinoma MCF-7 cells, *Anticancer Res.* 29 (2009) 2993-2996.
- [38] (a) P. Prayong, S. Barusrux, N. Weerapreeyakul, Cytotoxic activity screening of some indigenous Thai plants, *Fitoterapia*, 79 (2008) 598-601; (b) W. Mahavorasirikul, V. Viyanant, W. Chaijaroenkul, A. Itharat, K. Na-Bangchang, Cytotoxic activity of Thai medicinal plants against human cholangiocarcinoma, laryngeal and hepatocarcinoma cells in vitro, *BMC Complem. Altern. M.* 10 (2010) 55.
- [39] C.A. Lipinski, F. Lombardo, B.W. Dominy, P.J. Feeney, Experimental and computational approaches to estimate solubility and permeability in drug discovery and developments settings, *Adv. Drug Deliv. Rev.* 23 (1997) 3-25.

- [40] C.A. Lipinski, Lead- and drug-like compounds: the rule-of-five revolutions, *Drug Discov. Today Technol.* 1 (2004) 337–341.
- [41] D.F. Veber, S.R. Johnson, H.-Y. Cheng, B.R. Smith, K.W. Ward, K.D. Kopple, Molecular properties that influence the oral bioavailability of drug candidates, *J. Med. Chem.* 45 (2002) 2615–2623.
- [42] Software available free of charge at <http://www.molinspiration.com>. (retrieved on July 27th, 2019).
- [43] J.E. Chipuk, J.C. Fisher, C.P. Dillon, R.W. Kriwacki, T. Kuwana, D.R. Green, Mechanism of apoptosis induction by inhibition of the anti-apoptotic BCL-2 proteins, *Proc. Natl. Acad. Sci.* 105 (2008) 20327–20332.
- [44] S. Cory, J.M. Adams, The Bcl2 family: regulators of the cellular life-or-death switch, *Nat. Rev. Cancer.* 2 (2002) 647.
- [45] T. Moldoveanu, A.V. Follis, R.W. Kriwacki, D.R. Green, Many players in BCL-2 family affairs, *Trends Biochem. Sci.* 39 (2014) 101–111.
- [46] Y.-X. Ma, Z. Guo, T. Sun, CGRP inhibits norepinephrine induced apoptosis with restoration of Bcl-2/Bax in cultured cardiomyocytes of rat, *Neurosci. Lett.* 549 (2013) 130–134.
- [47] C. Zeng, Z. Ke, Y. Song, Y. Yao, X. Hu, M. Zhang, H. Li, J. Yin, Annexin A3 is associated with a poor prognosis in breast cancer and participates in the modulation of apoptosis in vitro by affecting the Bcl-2/Bax balance, *Exp. Mol. Pathol.* 95 (2013) 23–31.
- [48] L. Lalier, P.-F. Cartron, P. Juin, S. Nedelkina, S. Manon, B. Bechinger, F.M. Vallette, Bax activation and mitochondrial insertion during apoptosis, *Apoptosis*, 12 (2007) 887–896.
- [49] J. Neuzil, X.-F. Wang, L.-F. Dong, P. Low, S.J. Ralph, Molecular mechanism of ‘mitocan’-induced apoptosis in cancer cells epitomizes the multiple roles of reactive oxygen species and Bcl-2 family proteins, *FEBS Lett.* 580 (2006) 5125–5129.
- [50] F. Faião-Flores, P.R.P. Coelho, J.D.T. Arruda-Neto, S.S. Maria-Engler, M. Tiago, V.L. Capelozzi, R.R. Giorgi, D.A. Maria, Apoptosis through Bcl-2/Bax and cleaved caspase up-regulation in melanoma treated by boron neutron capture therapy, *PLoS One*, 8 (2013) e59639.
- [51] G.P. Dotto, J. Silke, More than cell death: caspases and caspase inhibitors on the move, *Dev. Cell.* 7 (2004) 2–3.
- [52] M. Redza-Dutordoir, D.A. Averill-Bates, Activation of apoptosis signalling pathways by reactive oxygen species, *BBA-Mol. Cell Res.* 1863 (2016) 2977–2992.
- [53] (a) DTP Human Tumor Cell Line Screen Process: https://dtp.cancer.gov/discovery_development/nci-60/methodology.htm. (retrieved on July 27th, 2019); (b) M.M.G. El-Din, M.I. El-Gamal, M.S. Abdel-Maksoud, K.H. Yoo, C.-H. Oh, Synthesis and in vitro anti-proliferative activity of new 1, 3, 4-oxadiazole derivatives possessing sulfonamide moiety, *Eur. J. Med. Chem.* 90 (2015) 45–52.
- [54] (a) E. Vega-Avila, M.K. Pugsley, An overview of colorimetric assay methods used to assess survival or proliferation of mammalian cells, *Proc. West. Pharmacol. Soc.* 54 (2011) 10–14; (b) P.W. Sylvester, Optimization of the tetrazolium dye (MTT) colorimetric assay for cellular growth and viability, *Drug Des. Discov. Humana Press.* 716 (2011) 157–168.

[55] H.J. Mauceri, N.N. Hanna, M.A. Beckett, D.H. Gorski, M.-J. Staba, K.A. Stellato, K. Bigelow, R. Heimann, S. Gately, M. Dhanabal, Combined effects of angiostatin and ionizing radiation in antitumour therapy, *Nature*, 394 (1998) 287-291.

[56] M.F. Tolba, A. Esmat, A.M. Al-Abd, S.S. Azab, A.E. Khalifa, H.A. Mosli, S.Z. AbdelRahman, A.B. Abdel-Naim, Caffeic acid phenethyl ester synergistically enhances docetaxel and paclitaxel cytotoxicity in prostate cancer cells, *Int. Union Biochem. Mol. Biol.* 65 (2013) 716–729.

Journal Pre-proof

Highlights:

- A new series of 1,2,3-triazole-chalcone hybrids has been synthesized and screened in vitro against a panel of NCI-60 human cancer cell lines.
- Compound **4d** with 3, 4-dimethoxyphenyl chalcone moiety was the most potent anticancer agent.
- Compound **4d** showed IC₅₀ values less than 1 μ M on 6 cancer cell lines with high Selectivity Index (SI).
- Compound **4d** induce cell cycle arrest in RPMI-8226 cell line at G2/M phase and trigger mitochondrial apoptotic pathway through accumulation of ROS, up regulation of BAX, down regulation of Bcl-2 and activation of caspases 3, 7, 9.

Declaration of interests

The authors declare that they have no known competing financial interests or personal relationships that could have appeared to influence the work reported in this paper.

The authors declare the following financial interests/personal relationships which may be considered as potential competing interests:

Journal Pre-proof